

Effect of Ageing Temperature on Localised Corrosion and Atmospheric Stress Corrosion Cracking of 15-5PH Stainless Steel

ICorr Aberdeen –TWI webinar
26/09/23

Alyshia Keogh*¹, Anthony Cook¹, Emily Aradi¹, Zacharie Obadia², Phil Prangnell¹, Fabio Scenini¹

¹ University of Manchester, U.K.

² Airbus, Toulouse, France

* Alyshia.Keogh@Manchester.ac.uk

Contents

- Introduction
- Aims & objectives
- Material & Heat Treatments
- Experimental Techniques
- Results
 - Effect of Heat Treatment on Microstructure
 - Pitting Susceptibility
 - Passive Layer integrity
 - Electrochemical Noise
 - Atmospheric cracking
- Summary & Conclusions

Introduction

Maraging Steels

= martensitic + ageing

Properties

- High strength
- Good ductility
- Reasonable corrosion resistance

Applications

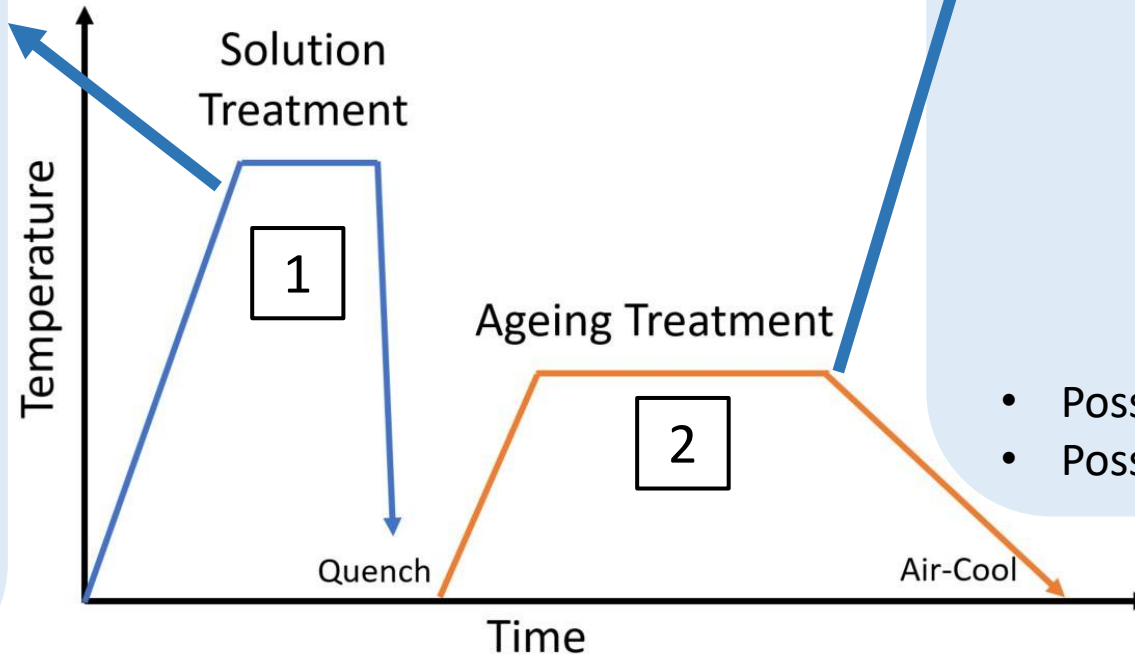
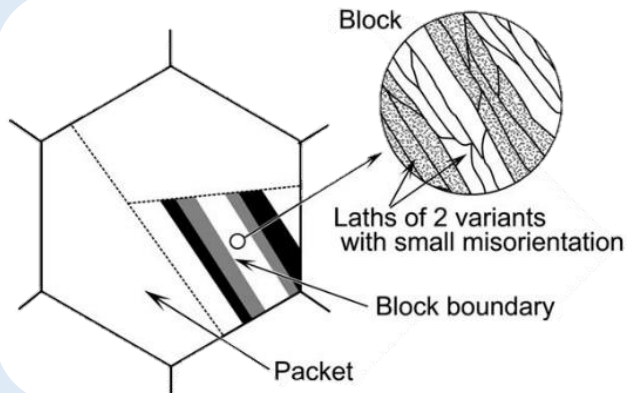
- Oil and Gas
- Aerospace



Introduction

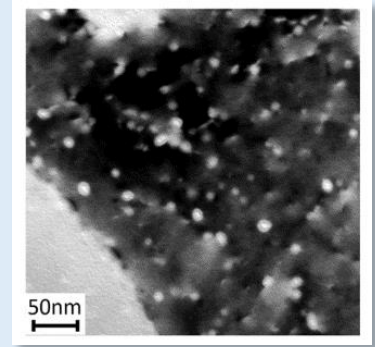
1

Solution treatment ~ 1038 °C ~ 1 hr
Obtain fully martensitic microstructure (& small amounts of **retained austenite**)



2

Ageing treatment ~ Lower Temperature)
• Form fine intermetallic precipitates



- Possible **austenite** reversion
- Possible **carbide** formation

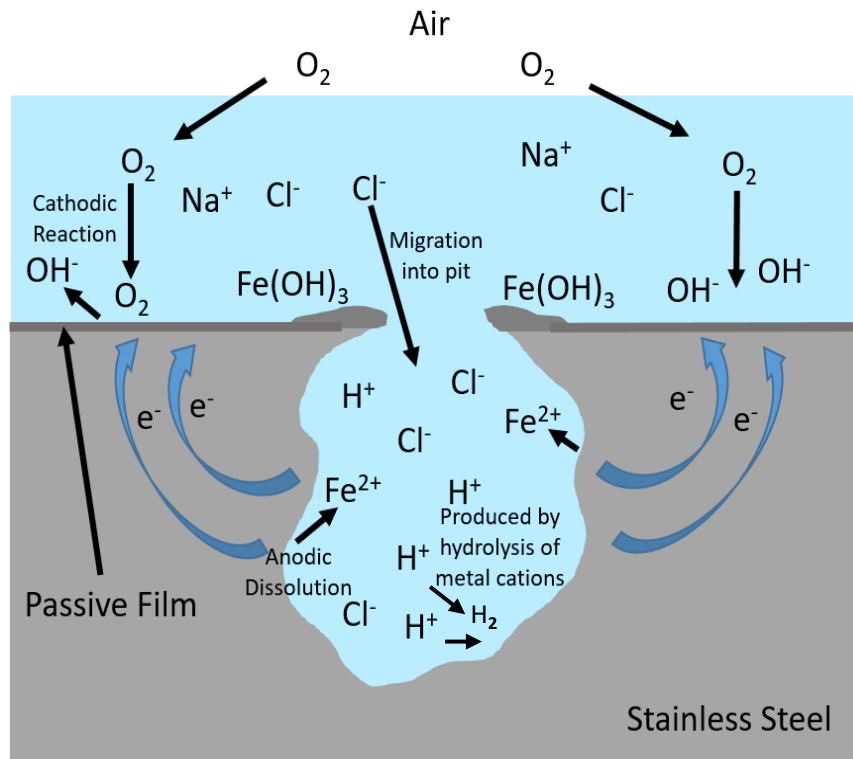
Schematic of typical heat treatment (not to scale)

Introduction

Problem:

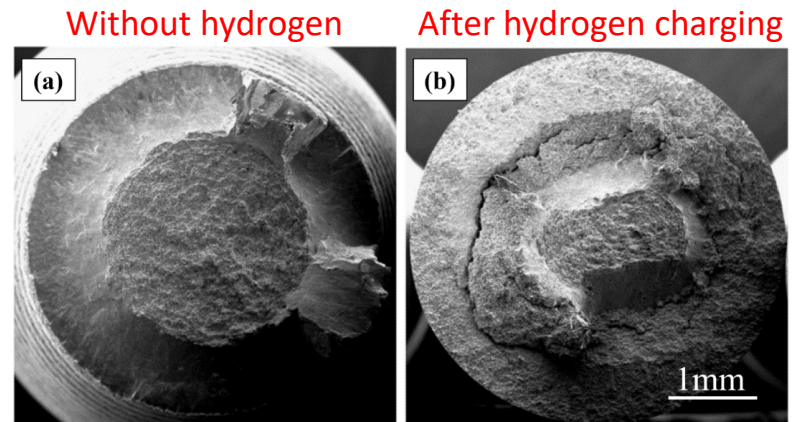
Maraging steels can be susceptible to **Localised Corrosion** (pitting or crevice corrosion) under certain conditions, which can be a precursor to **Environmentally Assisted Cracking (EAC)**; **chloride-induced Stress Corrosion Cracking (SCC)** and/or **Hydrogen Embrittlement (HE)**

Pitting – accelerated corrosion within localised cavity resulting from increased acidity through hydrolysis of metal ions

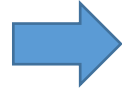


Hydrogen Embrittlement causes...

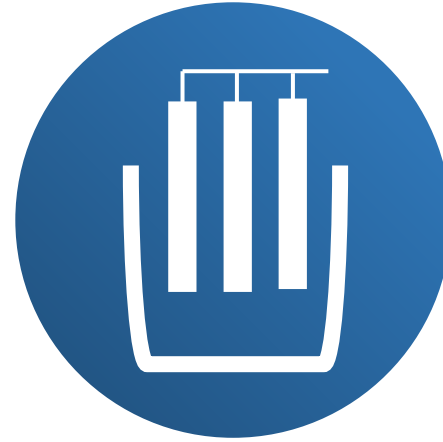
- Loss of tensile ductility
- Reduction in fracture toughness
- Catastrophic failure



Aims & Objectives



1. Characterise microstructure as a function of ageing treatment



2. Assess localised corrosion behavior of each microstructure



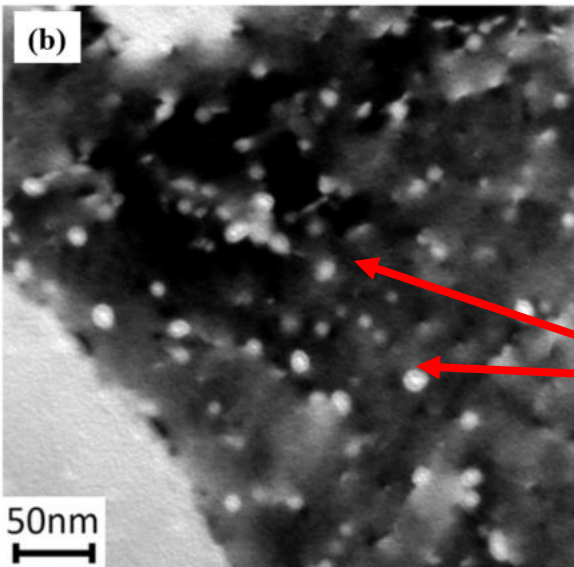
3. Link microstructural features to localized corrosion susceptibility

Understand the effect of microstructure on localised corrosion of 15-5PH to aid the design of future alloys

Material Composition

15-5 PH

Element	Fe	C	Cr	Ni	Cu	Mn	Si	Mo	Nb
Wt %	Bal	0.018	14.7	4.88	3.09	0.745	0.398	0.259	0.195



(1)

- Forms **Cu** Strengthening precipitates during ageing
- Increased levels of reverted austenite also expected as ageing temperature increased

Cu precipitates

Heat Treatment

1. Solution Treatment – 1 hr at 1038 °C
2. Ageing treatment – 4 hrs, varying temperature

Under-Aged 450 °C

Peak-Aged 540 °C

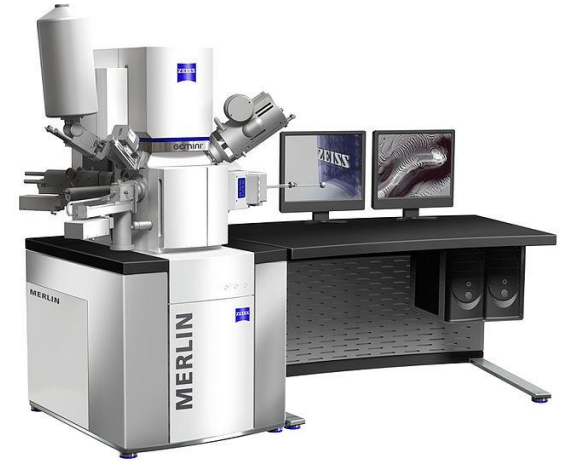
Over-Aged 650 °C

Experimental Techniques

Characterisation



- Mechanical Testing
 - Tensile properties
 - Hardness
- XRD
 - Austenite phase fraction
 - Based on methodology used by Tanaka and Choi (2003)
- Microscopy
 - SEM (Zeiss Sigma VP FEG)
 - TEM (ThermoFisher Talos F200X)



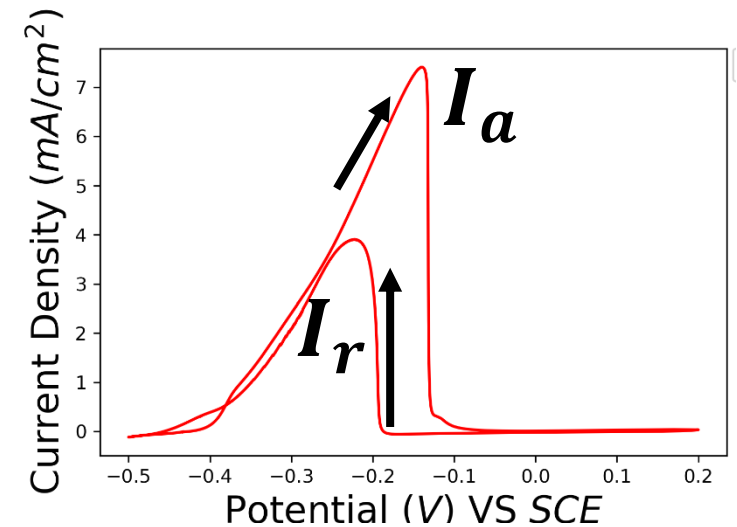
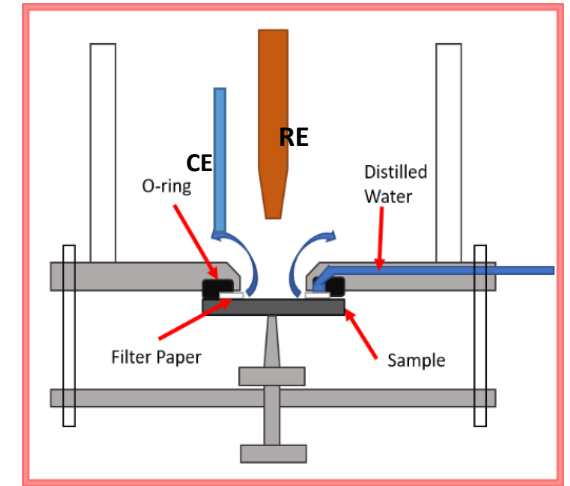
Experimental Techniques

Localised Corrosion

Electrochemical investigation of pitting susceptibility and reactivation behaviour



- Potentiodynamic Polarisation
 - Pitting susceptibility
- DL-EPR
 - Assessment of passive film integrity after heat treatment
- Electrochemical noise
 - Directly comparing microstructures



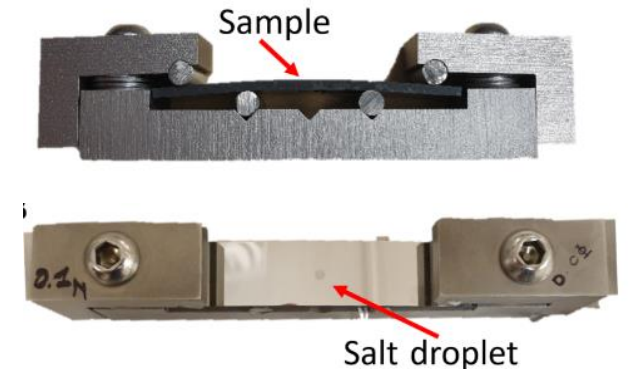
Experimental Techniques

Atmospheric Cracking

Study pit to crack transition and investigate cracking behaviour



- MgCl_2 salt deposits droplets
- Relative humidity (RH) of 30% or 90% in environmental chamber
- 50 °C
- Test performed over 5 or 10 days
- Surface features of crack and crack cross-section analysed by SEM post test

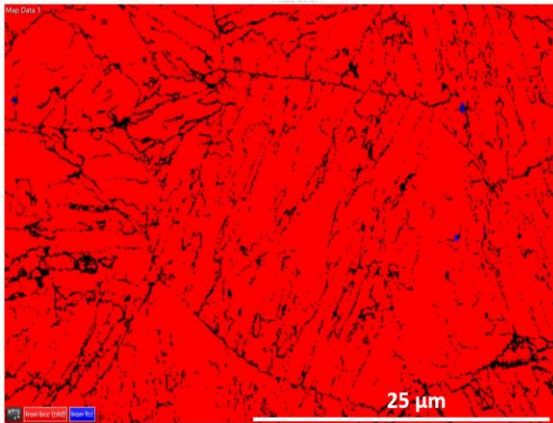


Results

Austenite Phase Fraction

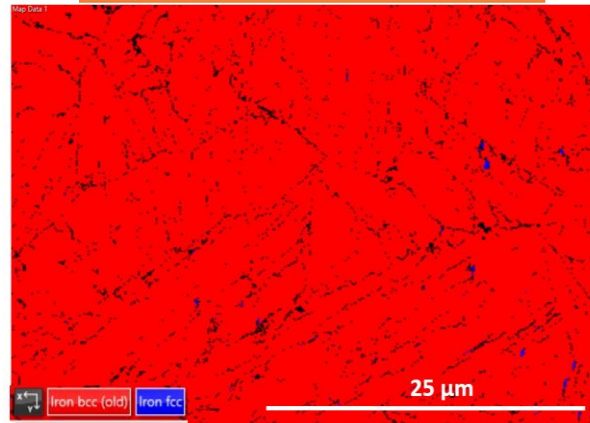
EBSD Phase maps

450 °C – Under-aged

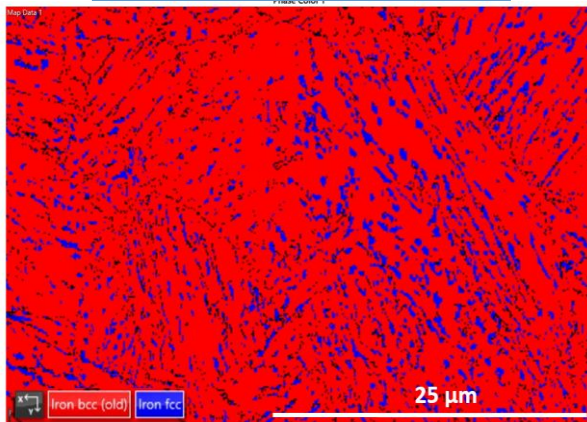


- α -martensite
- γ -austenite

540 °C – Peak-aged

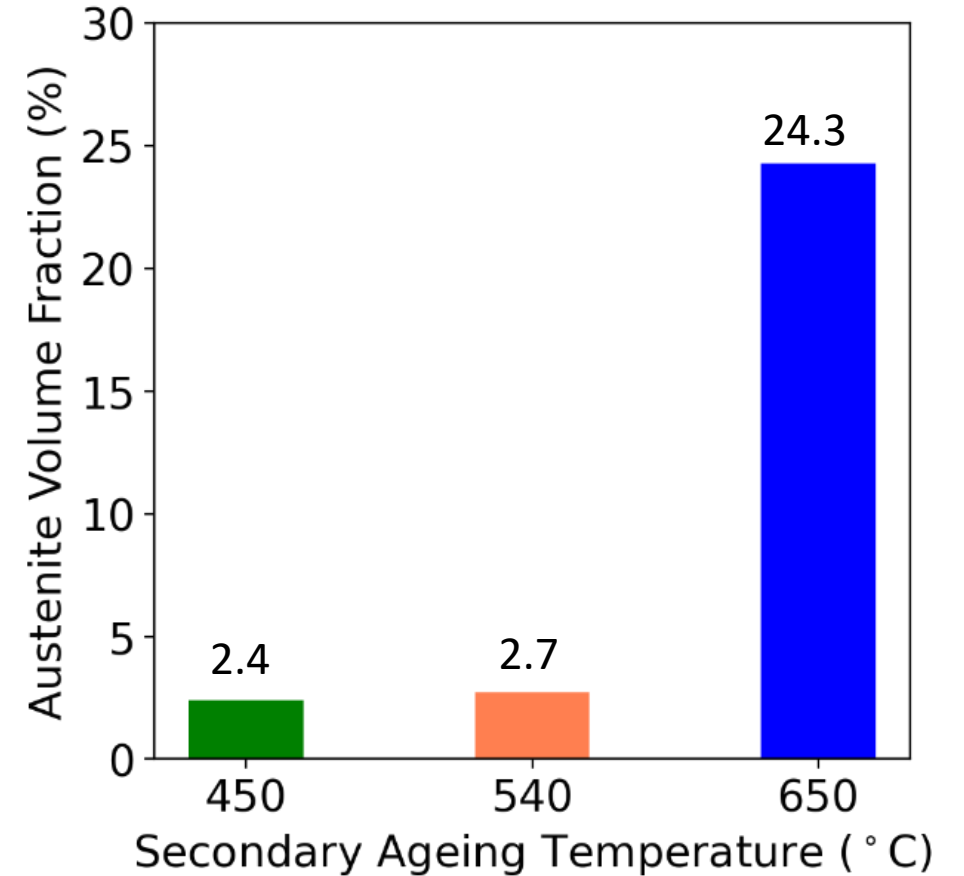


650 °C – Over-aged

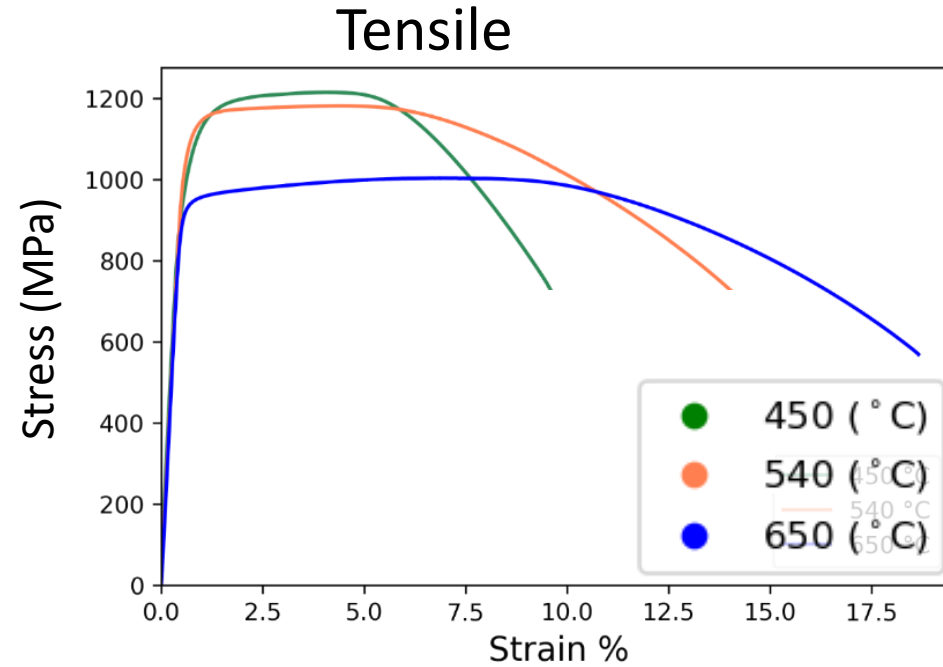
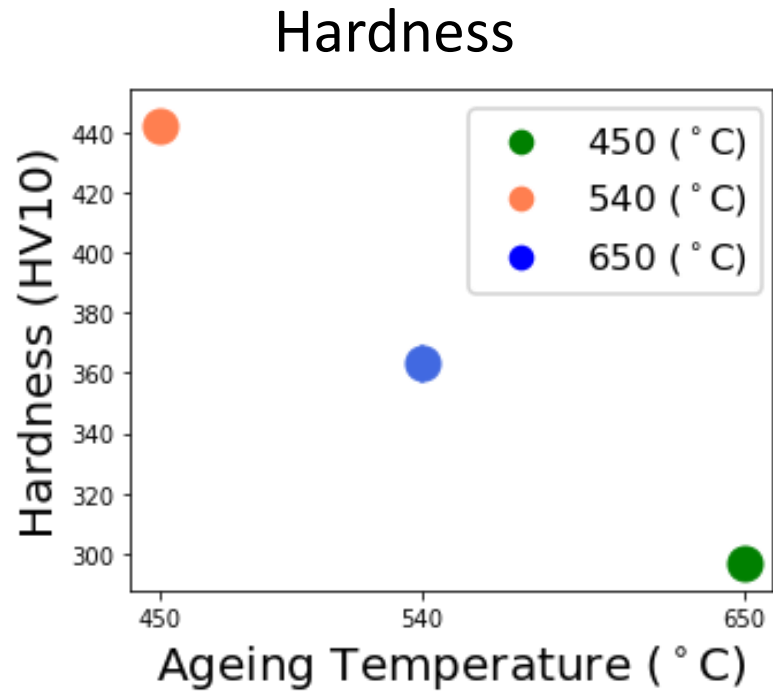


- Phase maps - qualitative measure of austenite content
- Austenite nucleates along lath boundaries and PAGBs
- Austenite reversion greatest with 650 °C ageing treatment

XRD Phase Fraction



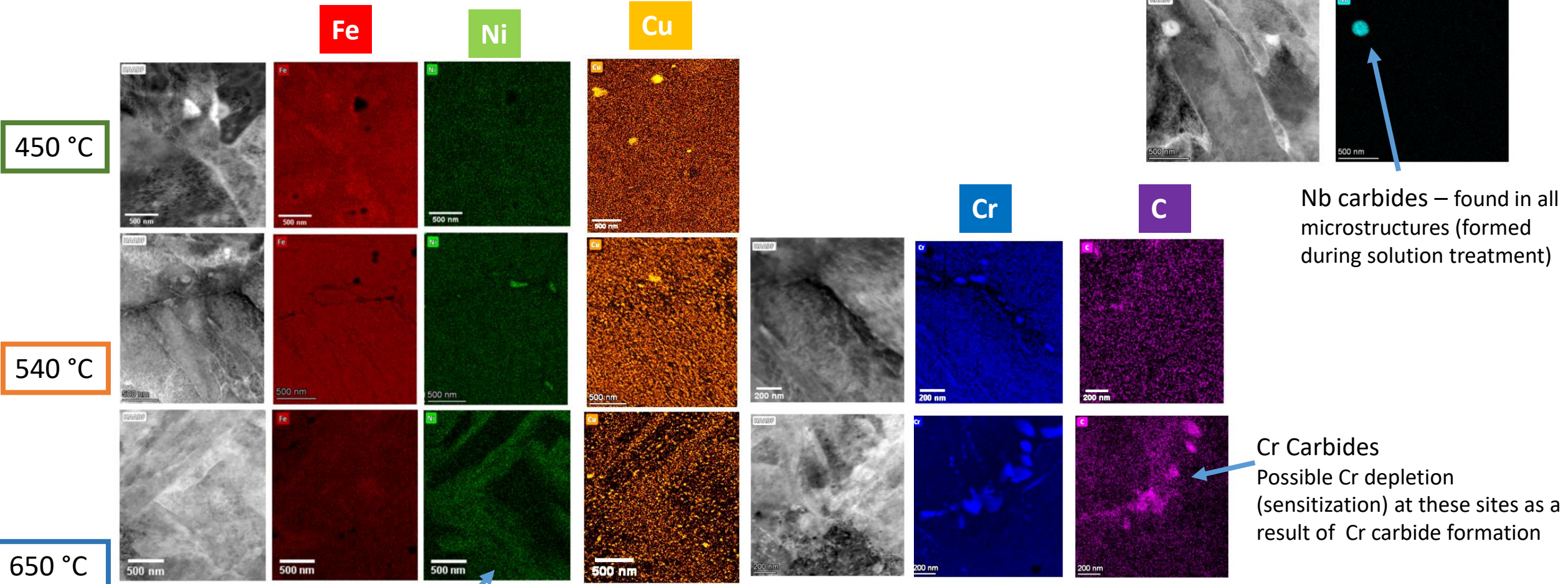
Mechanical Properties



- Increase in ageing temperature results in:
 - Decrease in hardness
 - Decrease in UTS
 - Increase in tensile ductility

Elemental Distribution as a Function of Aging Temperature

STEM EDX - allows characterisation of different aspects of the microstructure



Nb carbides – found in all microstructures (formed during solution treatment)

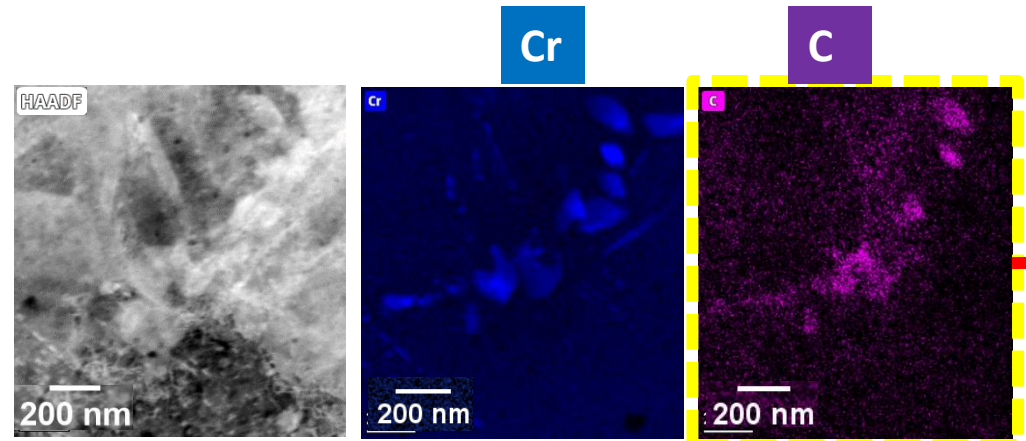
Cr Carbides
Possible Cr depletion (sensitization) at these sites as a result of Cr carbide formation

Increased Austenite content in 650 °C indicated by presence of Ni

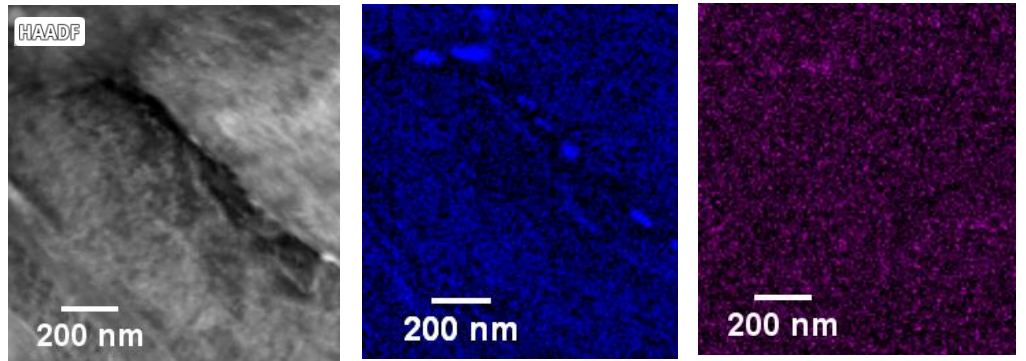
Coarsening of Cu Precipitates with increased aging temperature

Chromium Carbide Precipitation as a Function of Ageing Temperature

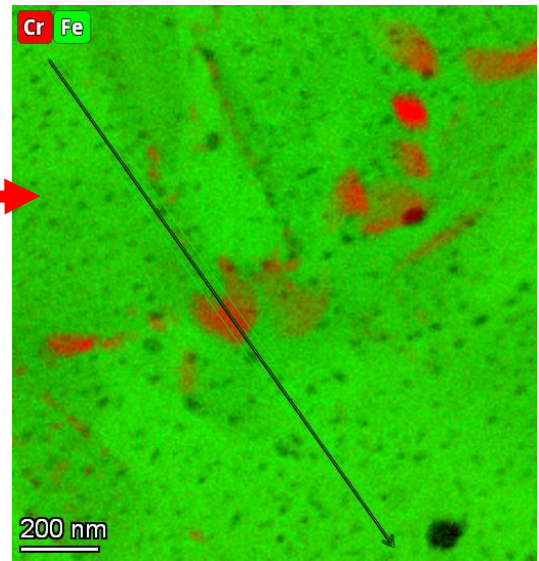
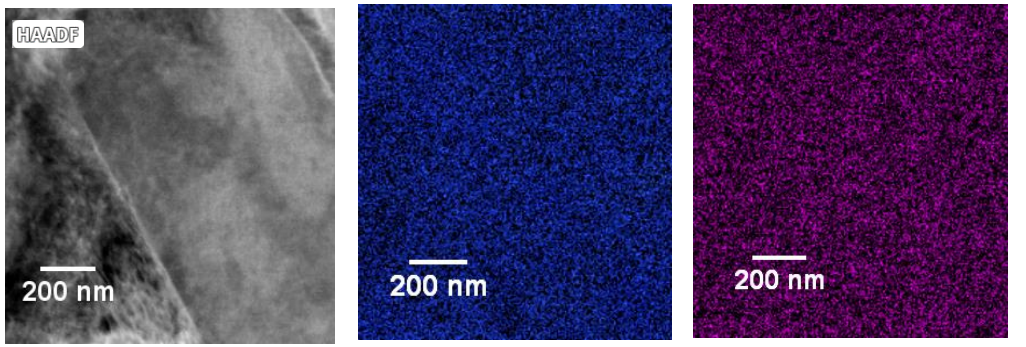
650 °C



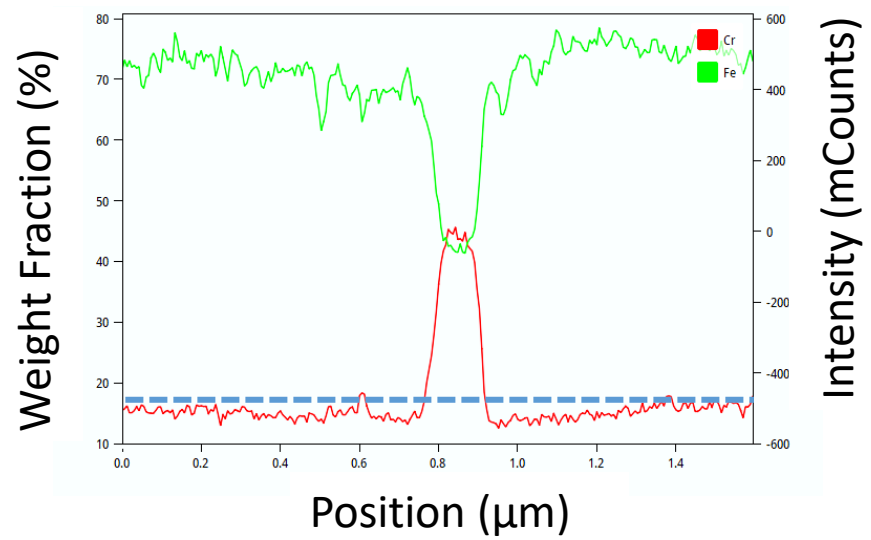
540 °C



450 °C

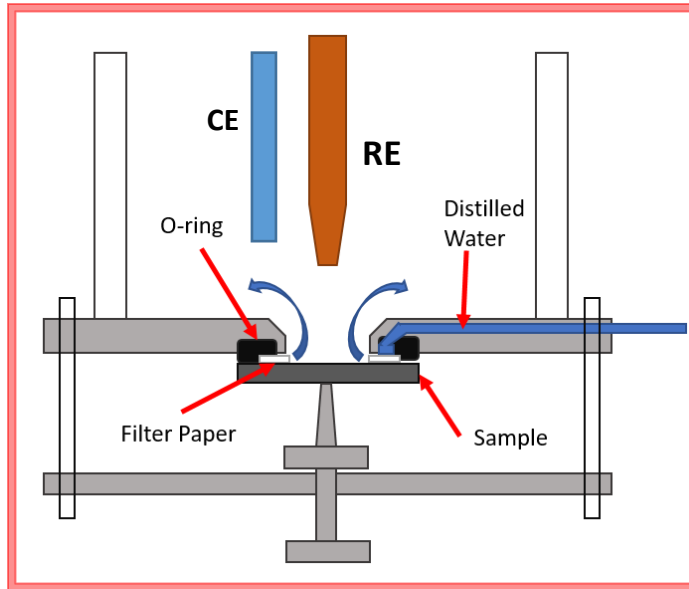


- Cr carbides found in 540 °C and 650 °C microstructures
- Line scan reveals slight Cr depletion around carbide in sample aged at 650 °C
 - Possible initiation site for localised corrosion

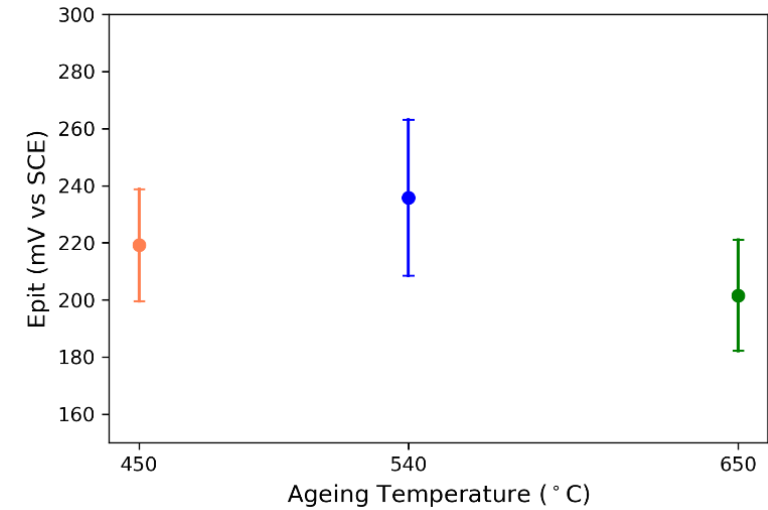
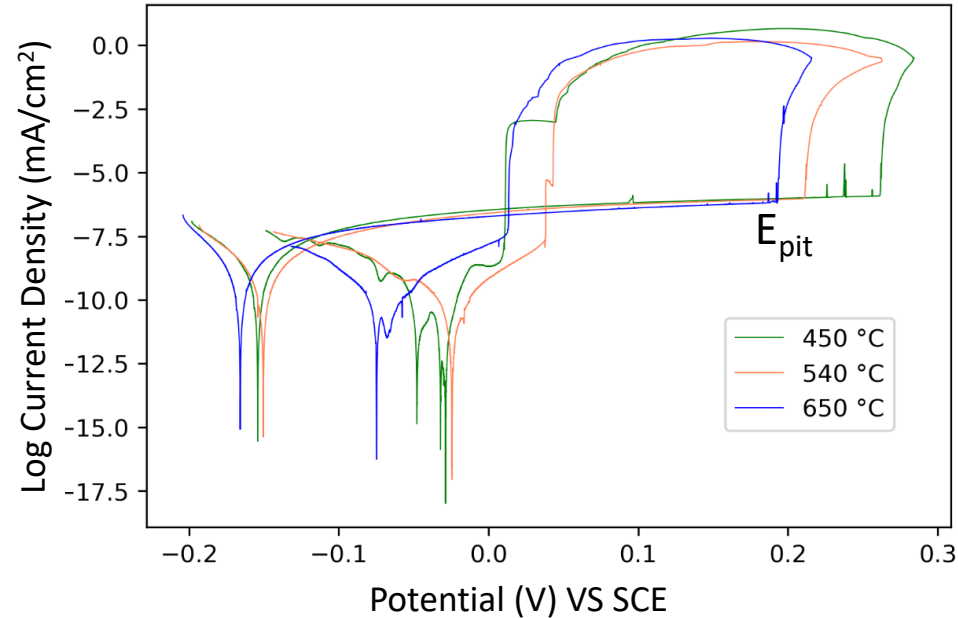


Microstructural Effects on Pitting Susceptibility

Tests conducted in an Avesta Cell
– Inhibits crevice corrosion



- 0.6 M NaCl
- 0.5 mV/s
- 1 μm diamond polish
- OCP measured for one hour



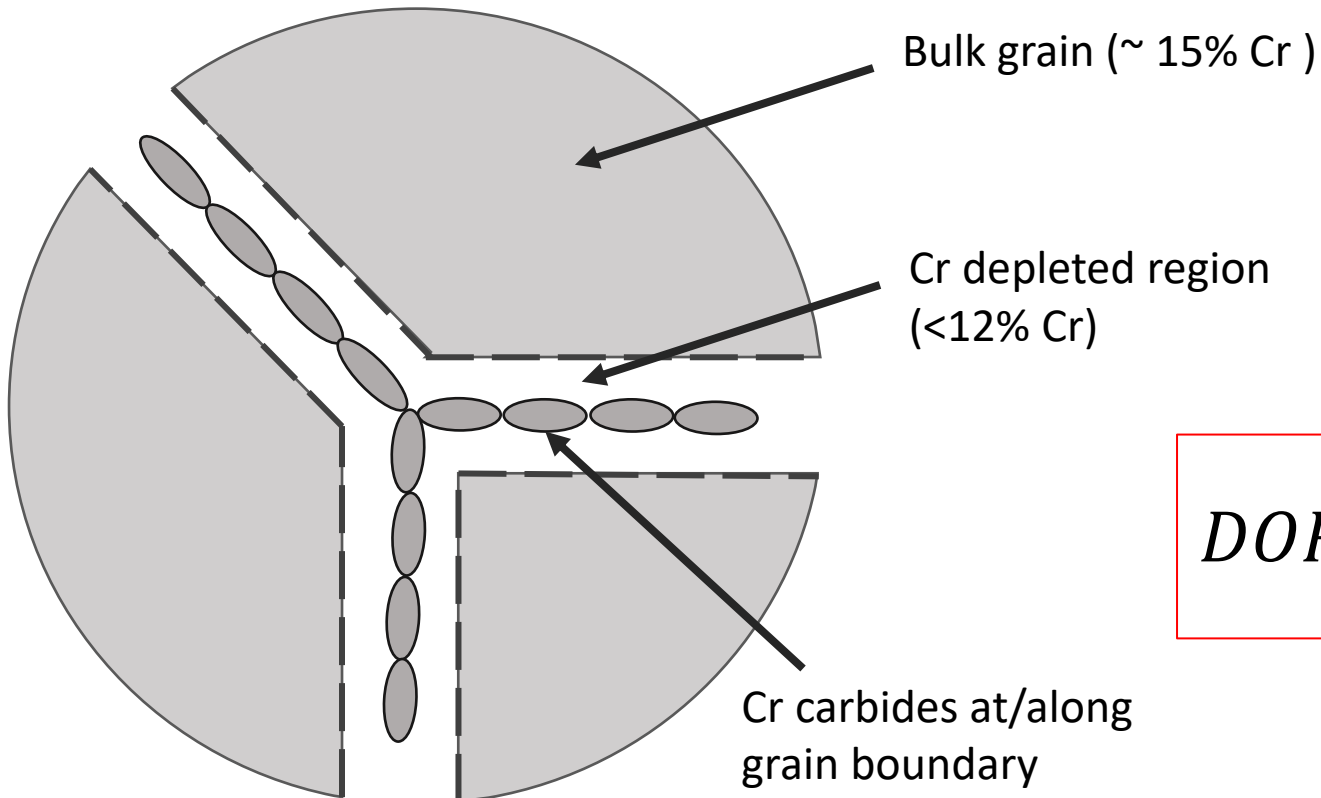
- On average 650 °C has the lowest E_{pit}
- However scatter is too large for E_{pit} to be considered statistically different
- Pitting is a stochastic process and PDP may not account for slight differences in microstructure

Effect of Aging Temperature on Passive Layer Integrity

DL-EPR (Double Loop Electrochemical Potentiokinetic Reactivation)

Technique detects degree of reactivation (DOR) in steels:

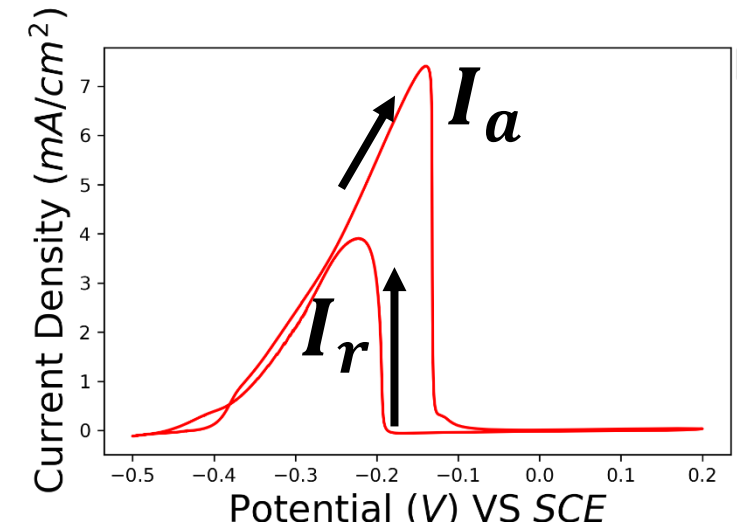
- Reactivation loop usually related to loss of passive film on grain boundaries where Cr depletion has lead to sensitization



$$DOR = \frac{I_r}{I_a}$$

Experimental Conditions:

- 0.25 M H₂SO₄ 0.01 M KSCN
- Scan rate: 0.5 mV/s
- 1200 grit surface finish



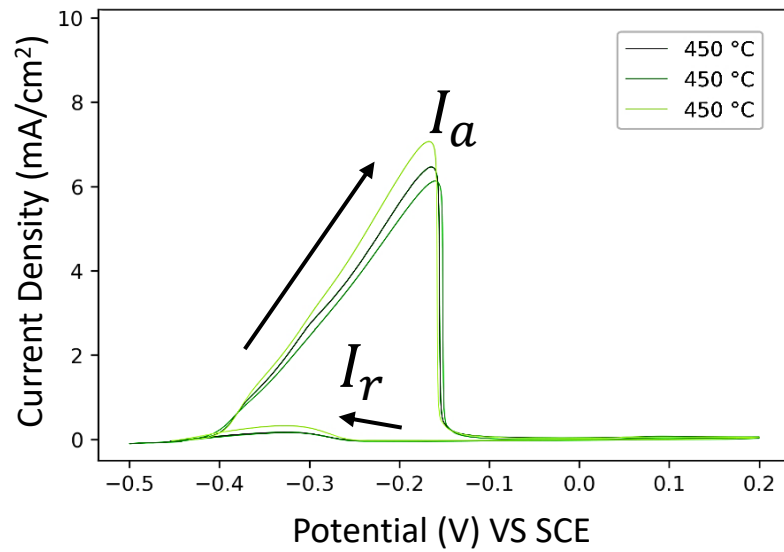
Effect of Aging Temperature on Passive Layer Integrity

DL-EPR

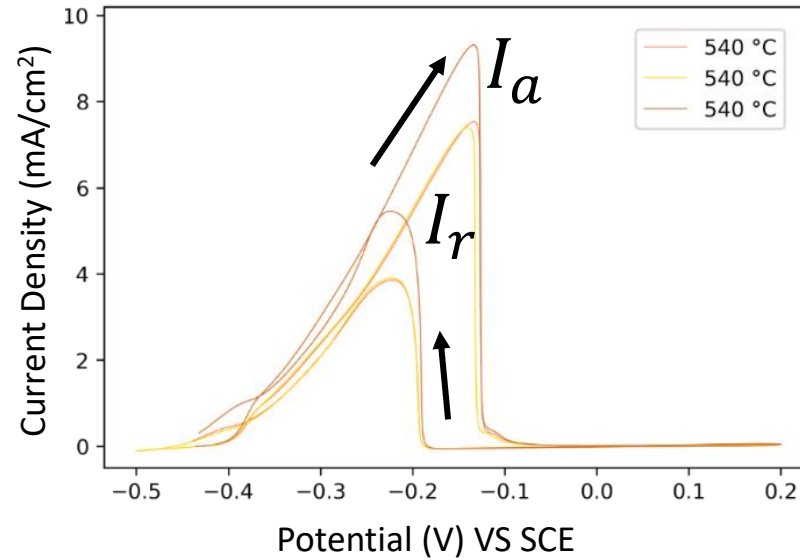
Experimental Conditions:

- 0.25 M H_2SO_4 0.01 M KSCN
- Scan rate: 0.5 mV/s
- 1200 grit surface finish

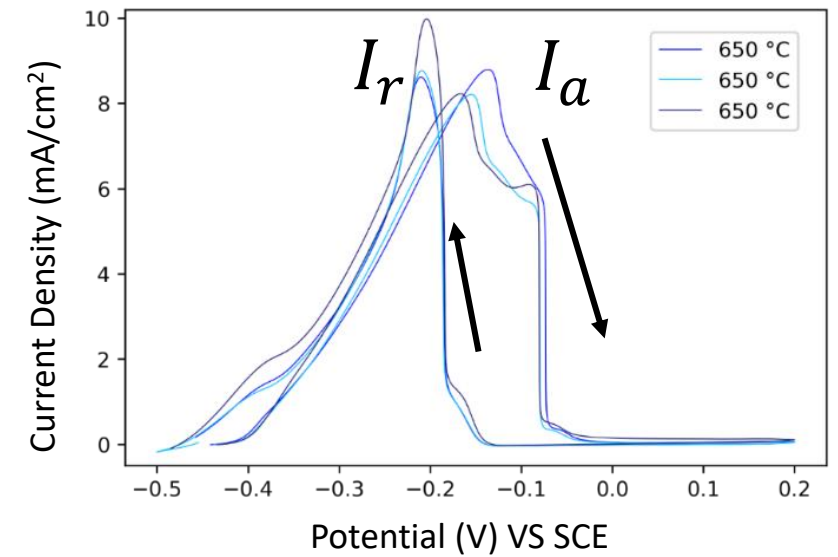
450 °C



540 °C



650 °C



Effect of Aging Temperature on Passive Layer Integrity

DL-EPR

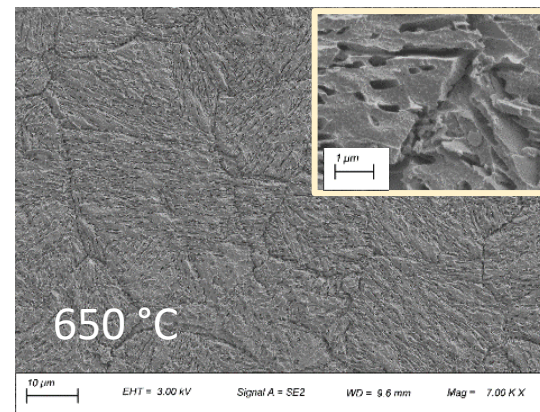
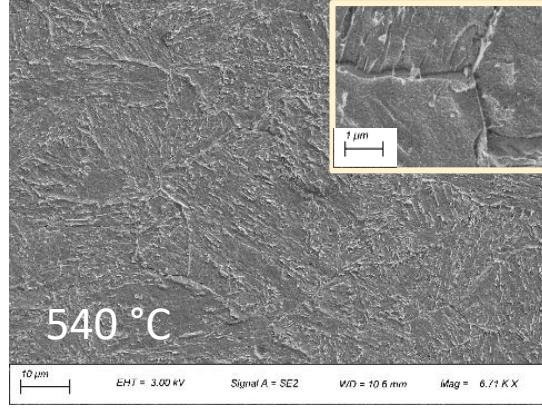
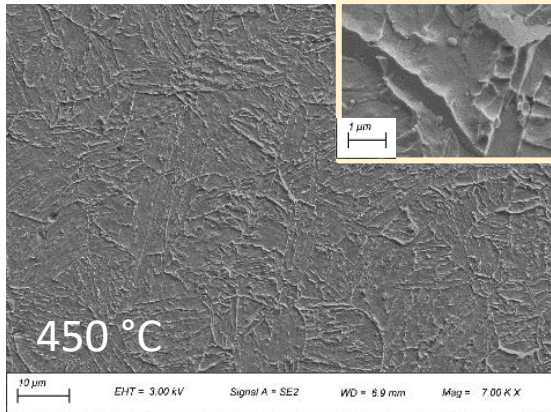
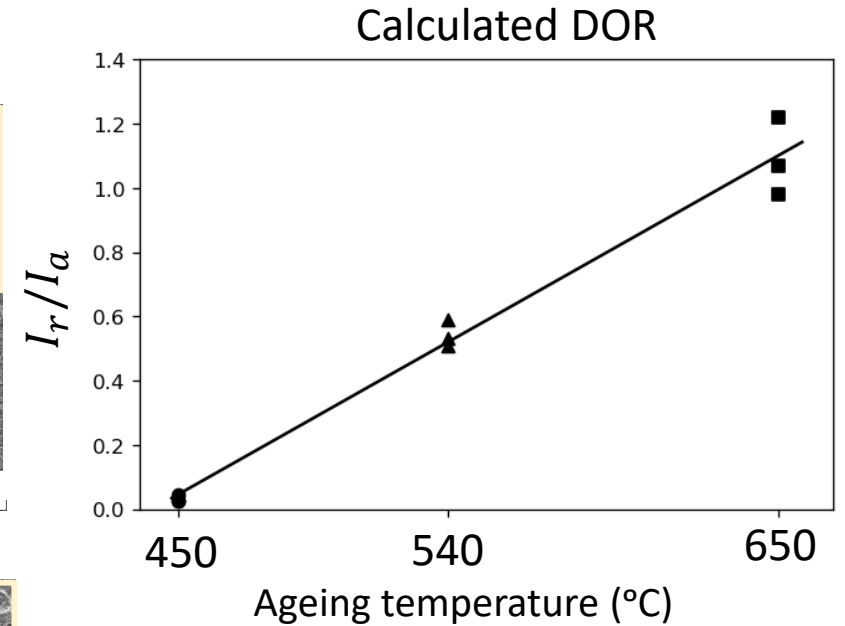
450 °C

540 °C

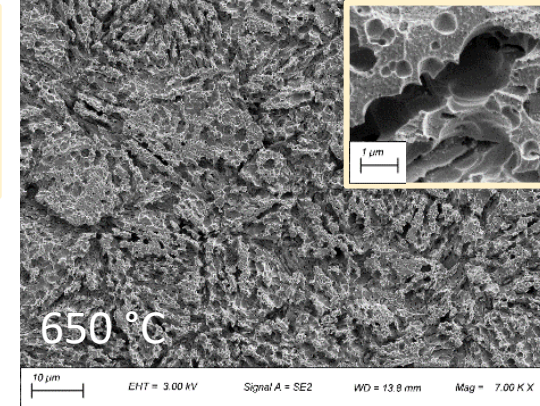
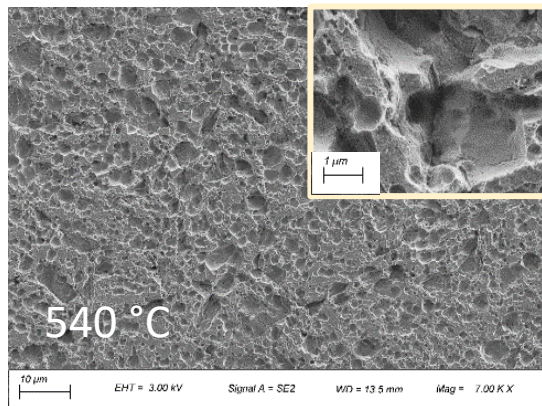
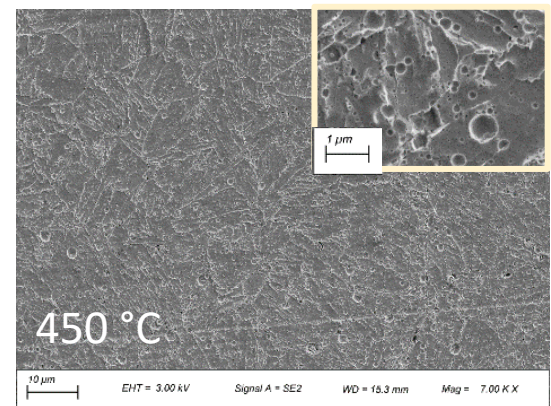
650 °C

- Experimental Conditions:
- 0.25 M H₂SO₄ 0.01 M KSCN
 - Scan rate: 0.5 mV/s
 - 1200 grit surface finish

After Anodic Scan



After Reverse Scan



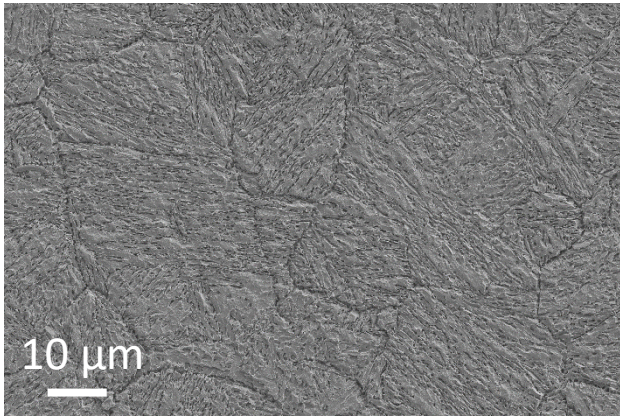
- Results are reproducible
- DOR increases with ageing temperature
- May be related to presence of Cr carbides in the microstructure

Effect of Aging Temperature on Passive Layer Integrity

650 °C

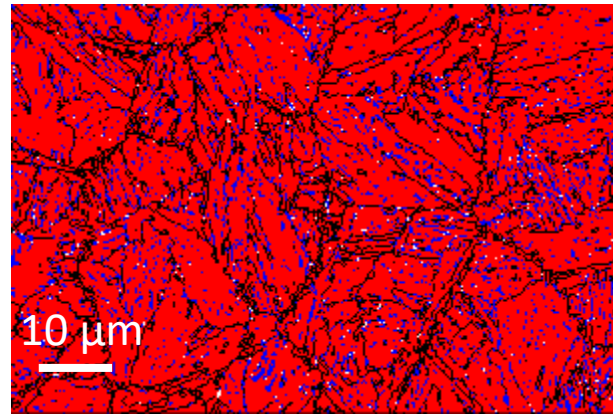
EBSD data

After anodic scan (DL-EPR)

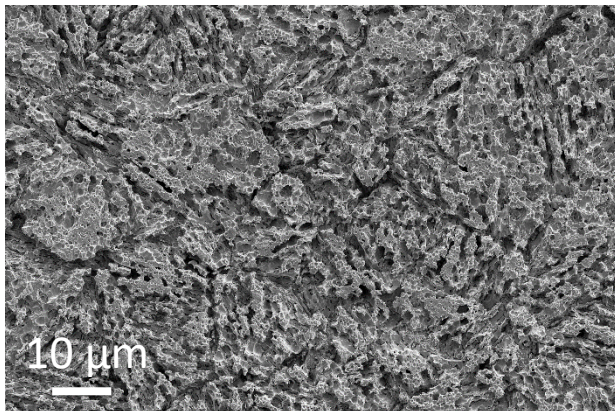


Phase fraction

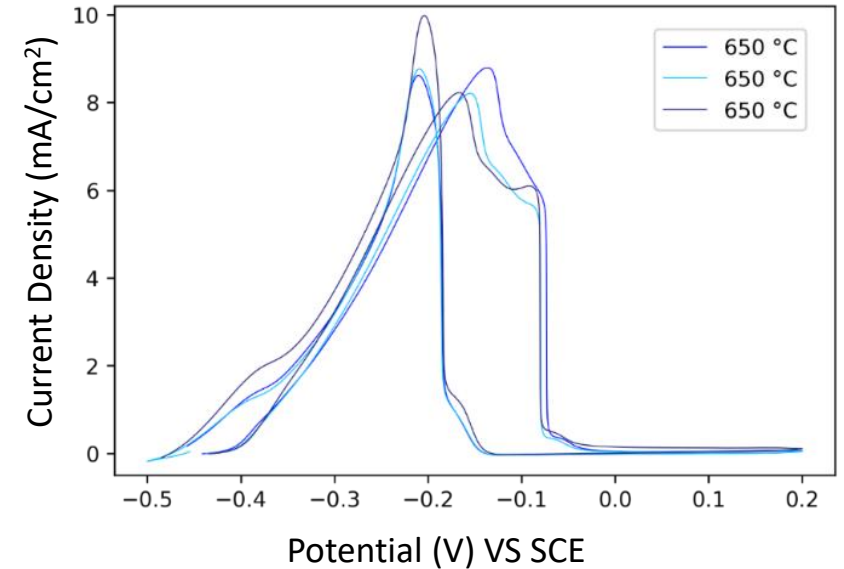
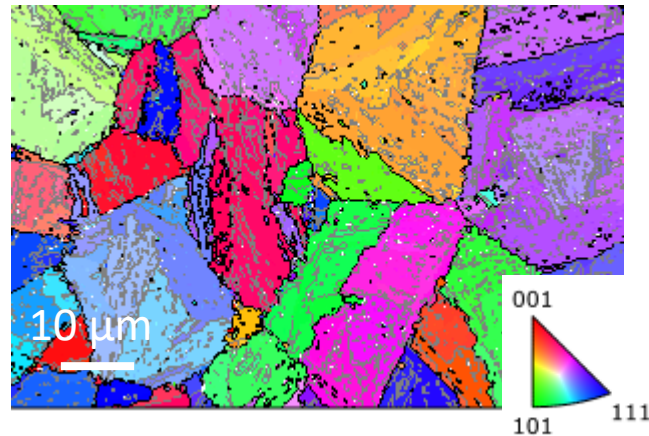
- α -martensite
- γ -austenite



After reverse scan (DL-EPR)



Reconstructed austenite grains

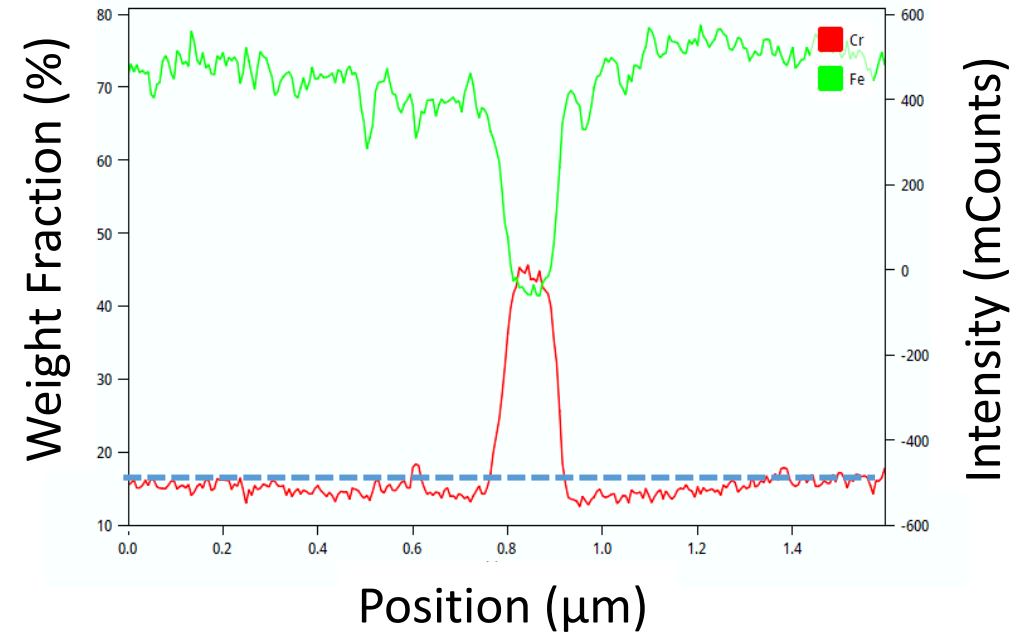
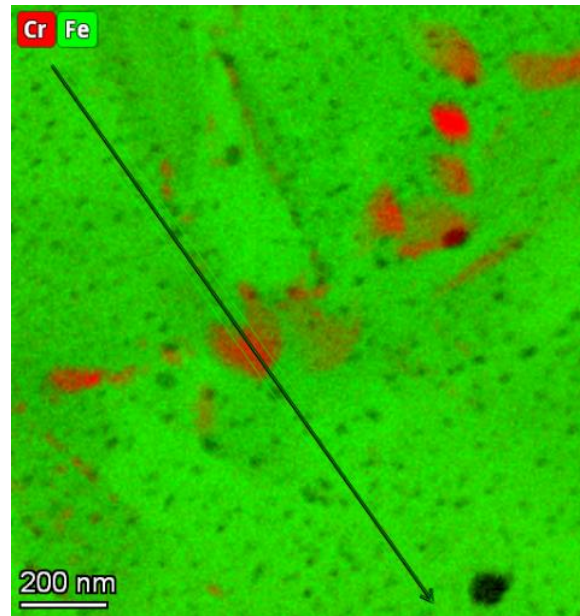
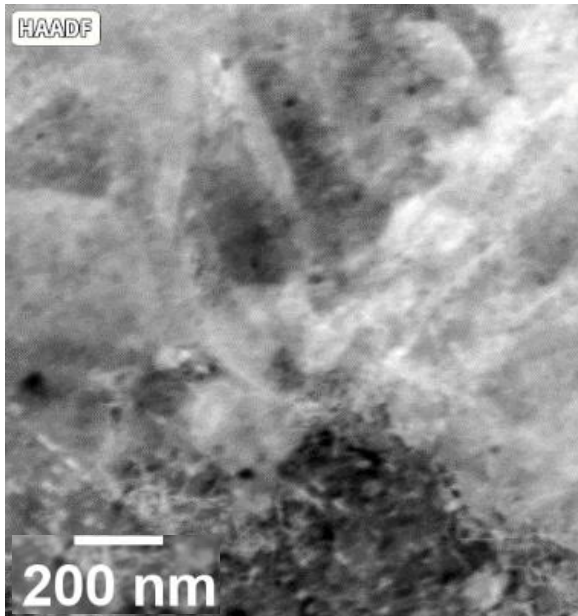


- Deeper etching along PAGBs
- High DOR measured through DL-EPR
 - Possible that reverted austenite has lower Cr content than matrix (1)

(1) L. Couturier, et al. *Materials and Design*, vol. 107, 2016

Effect of Aging Temperature on Passive Layer Integrity

650 °C



- Evidence of Cr depletion around Cr carbides
- High DOR in samples aged at 650 °C may be due to an increase in the heterogeneity of Cr in the microstructure, disrupting the passive film creating more initiation sites for localised corrosion

Effect of Aging Temperature on Passive Layer Integrity

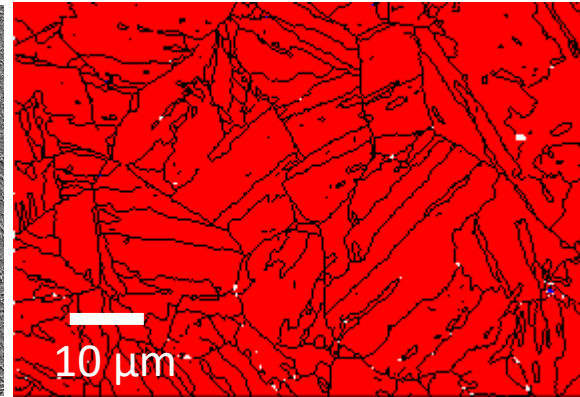
450 °C

EBSD data

- α -martensite
- γ -austenite

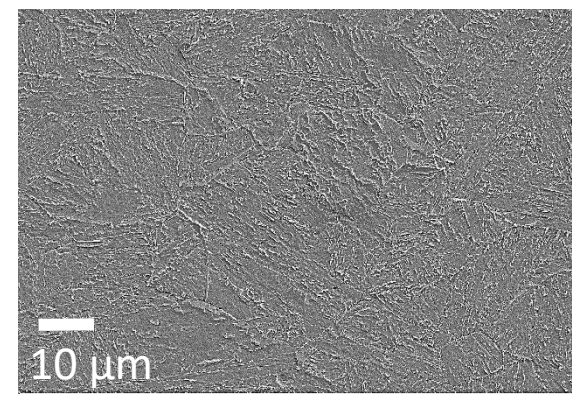
After anodic scan (DL-EPR)

Phase fraction



After anodic scan (DL-EPR)

Phase fraction



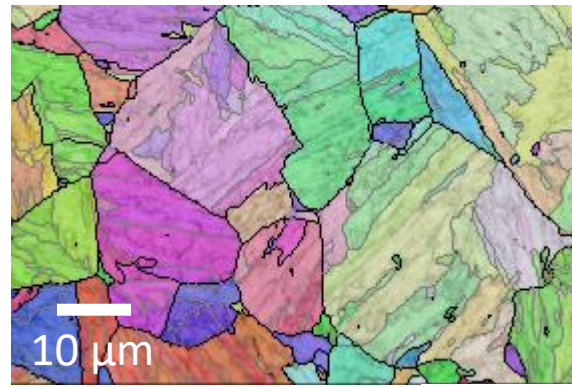
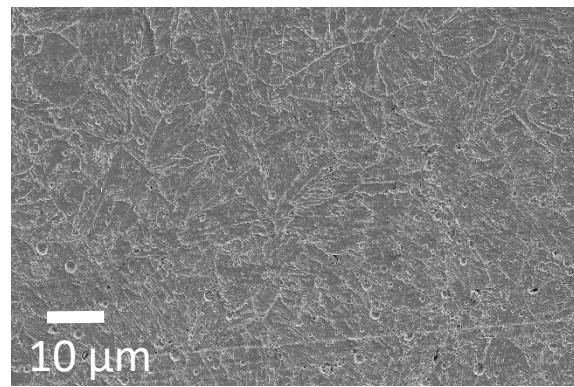
540 °C

EBSD data

- α -martensite
- γ -austenite

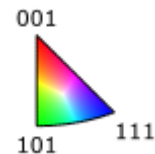
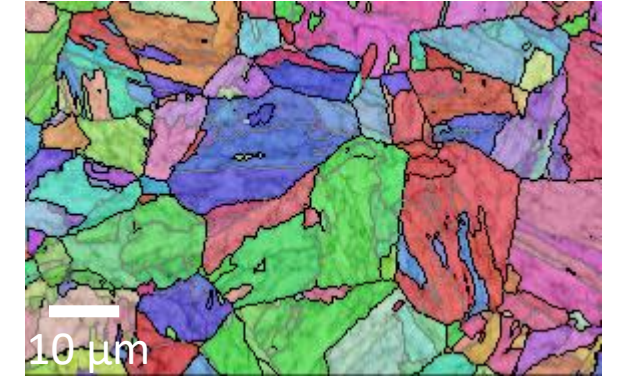
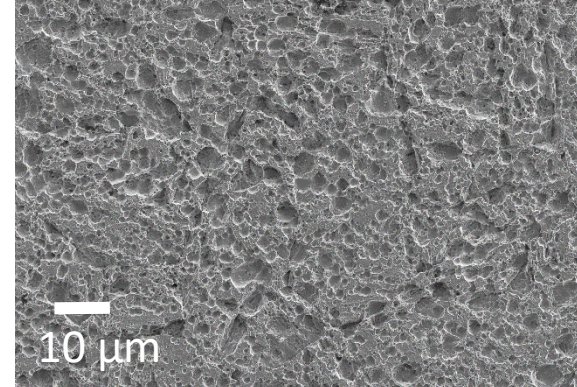
After reverse scan (DL-EPR)

Reconstructed austenite grains

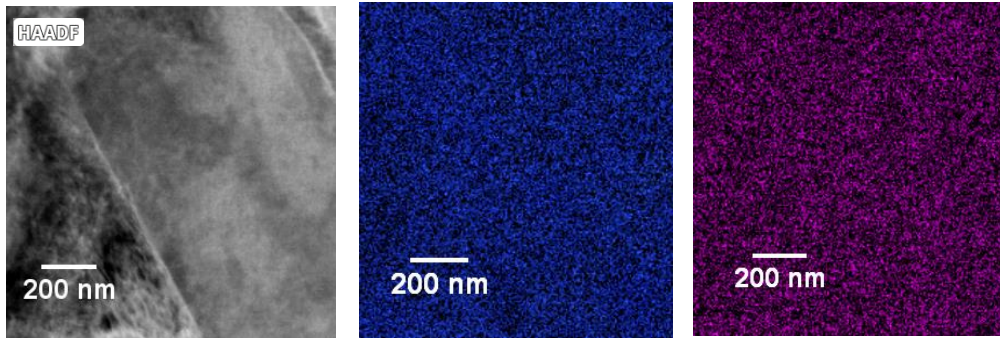
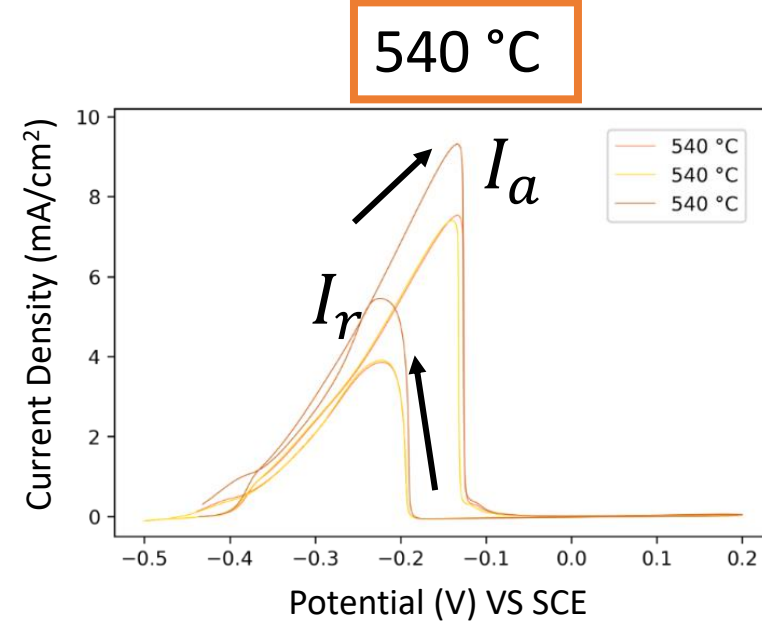
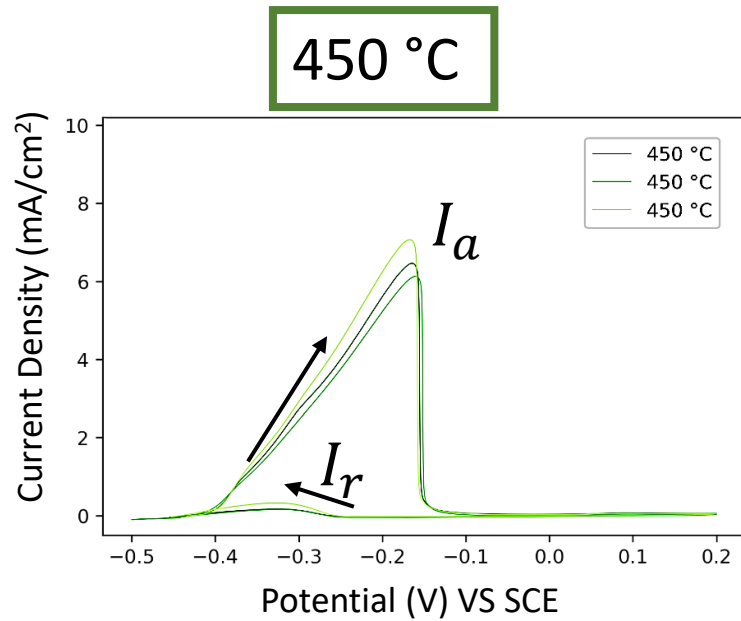


After reverse scan (DL-EPR)

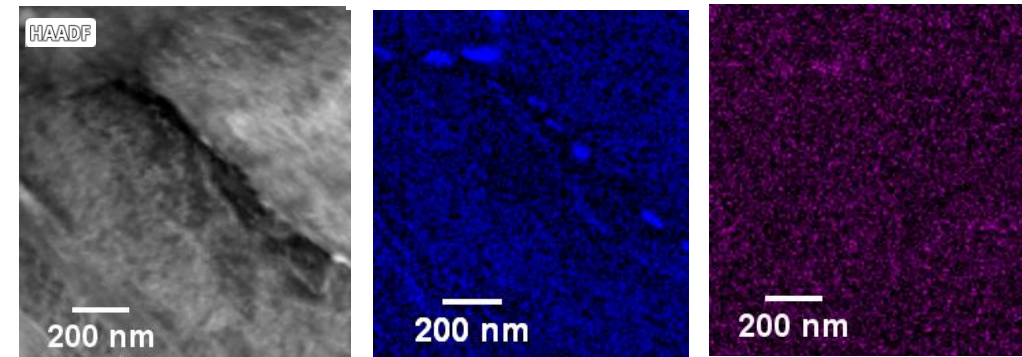
Reconstructed austenite grains



Effect of Aging Temperature on Passive Layer Integrity



- Low DOR – indicates more even distribution of Cr in the microstructure



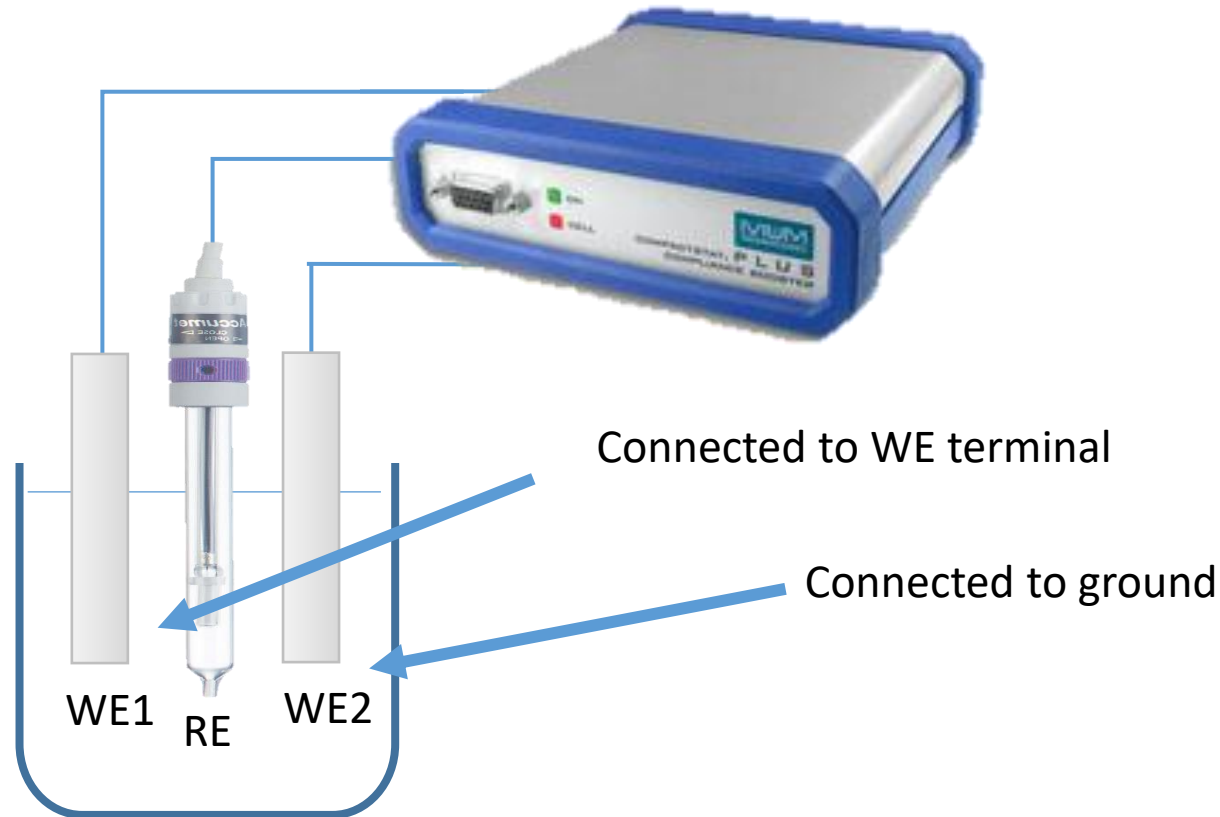
- Increase in DOR – Cr carbides found along GBs

Comparison of Pitting Susceptibility via Electrochemical Noise

ECN

- Direct comparison of pitting susceptibility in 2 different microstructures

Electrodes coupled via Compact Stat in ZRA configuration



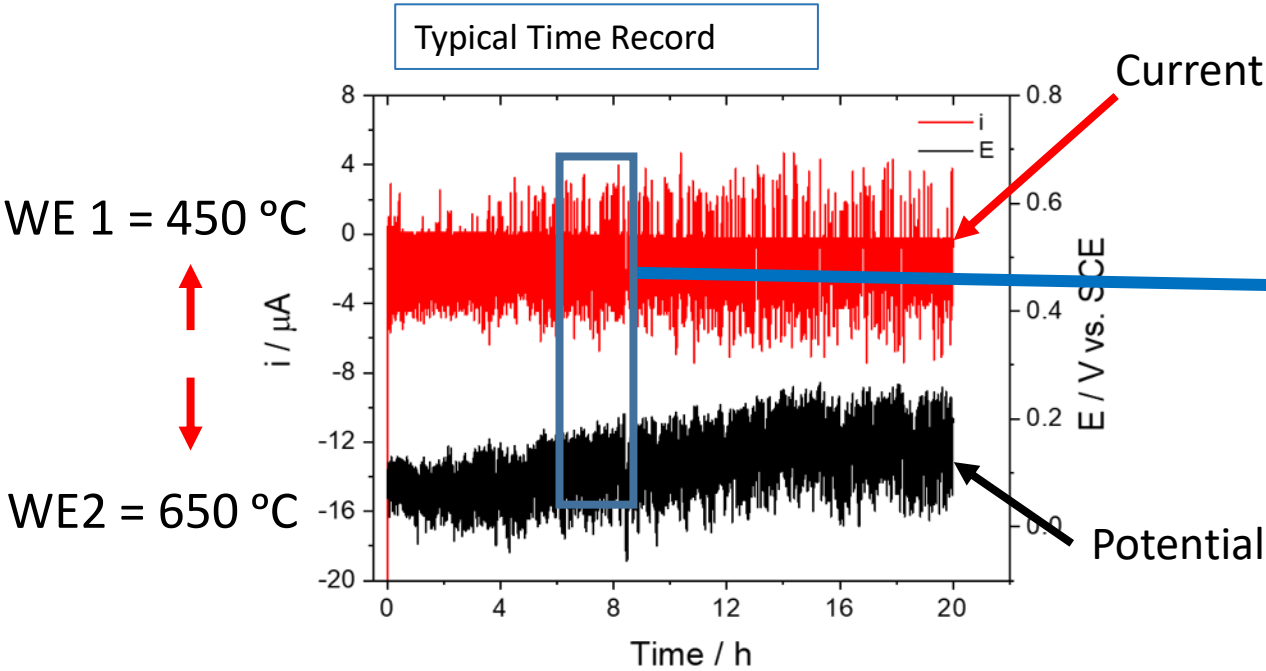
Experimental Conditions

- 0.15% FeCl₃ + NaCl (total Cl⁻ 0.6 M)
- Surface finish – 400 grit SiC

Resultant current transients resulting from metastable pitting measured

- +ve transients indicate pitting on WE1
- -ve transients indicate pitting on WE2

Comparison of Pitting Susceptibility via Electrochemical Noise

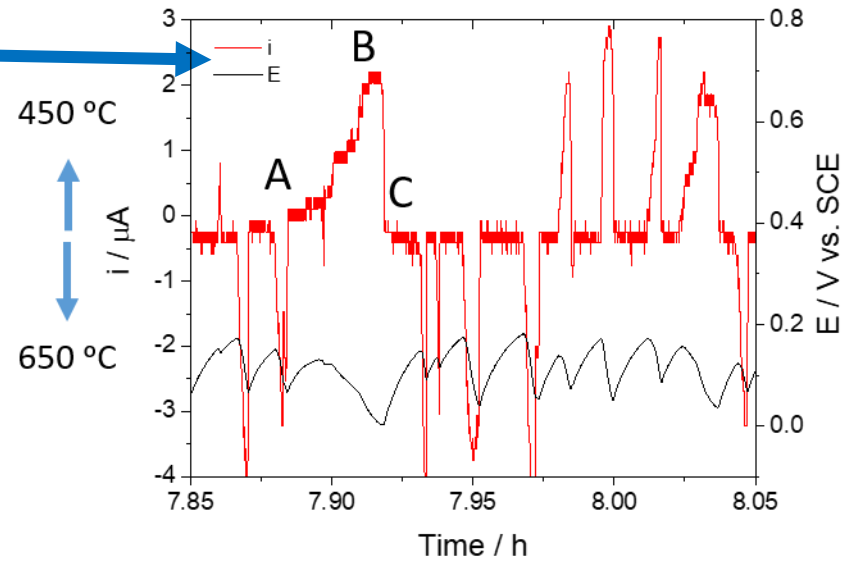


Experimental Conditions

- 0.15% FeCl₃ + NaCl (total Cl⁻ 0.6 M)
- Surface finish – 400 grit SiC

Note :

- +ve current indicates WE1 is pitting (450 °C sample)
- -ve current indicates WE2 is pitting (650 °C sample)



A - pit initiation on WE1 (450 °C)

A → B pit growth

B → C pit repassivation

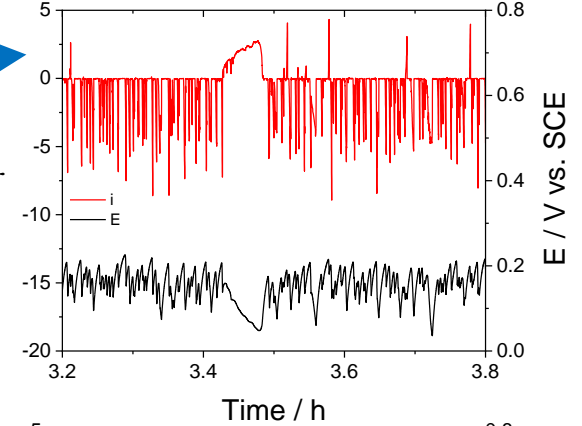
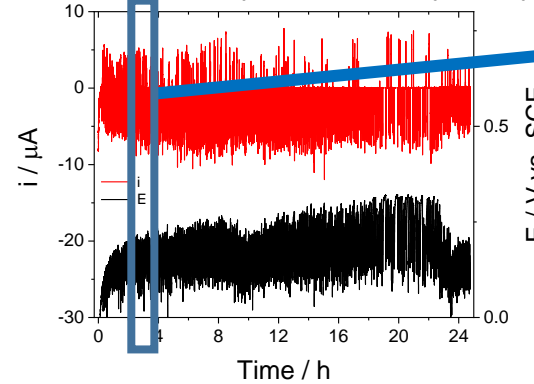
Potential drops when pit initiates and rises when pit repassivates

Comparison of Pitting Susceptibility via Electrochemical Noise

- More frequent metastable events on 650 °C compared to 450 °C

450 °C
↑
650 °C

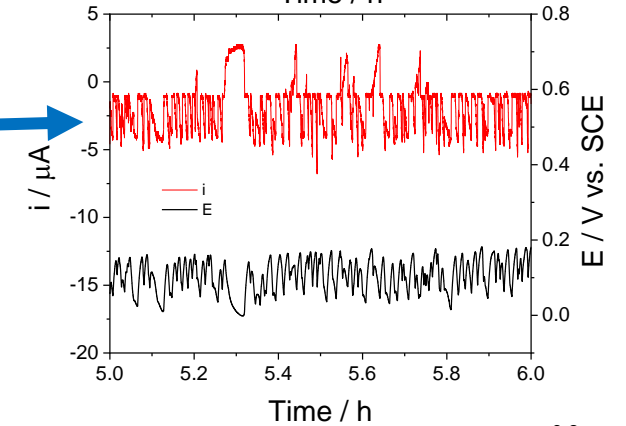
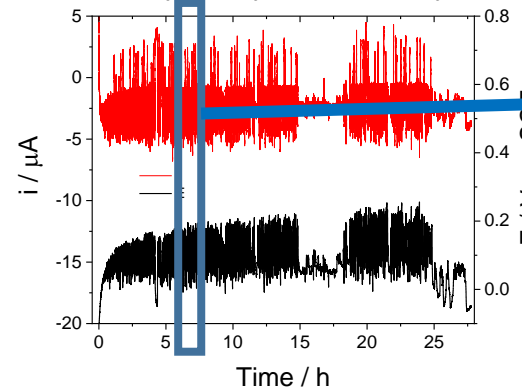
450 °C (WE1) + 650 °C (WE2)



- More frequent metastable events on 540 °C compared to 450 °C

450 °C
↑
540 °C

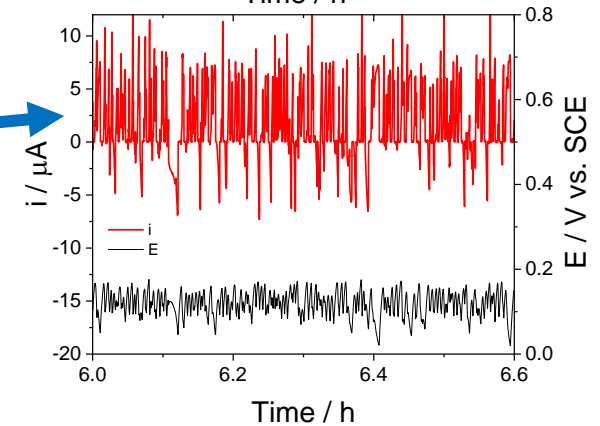
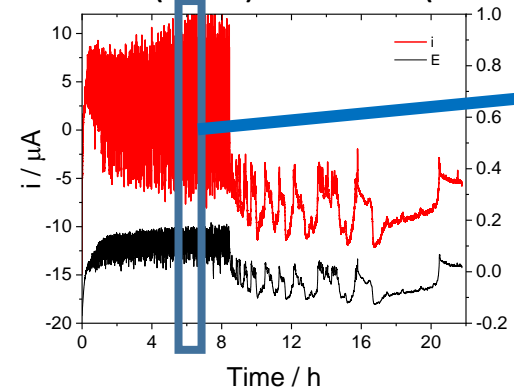
450 °C (WE1) + 540 °C (WE2)



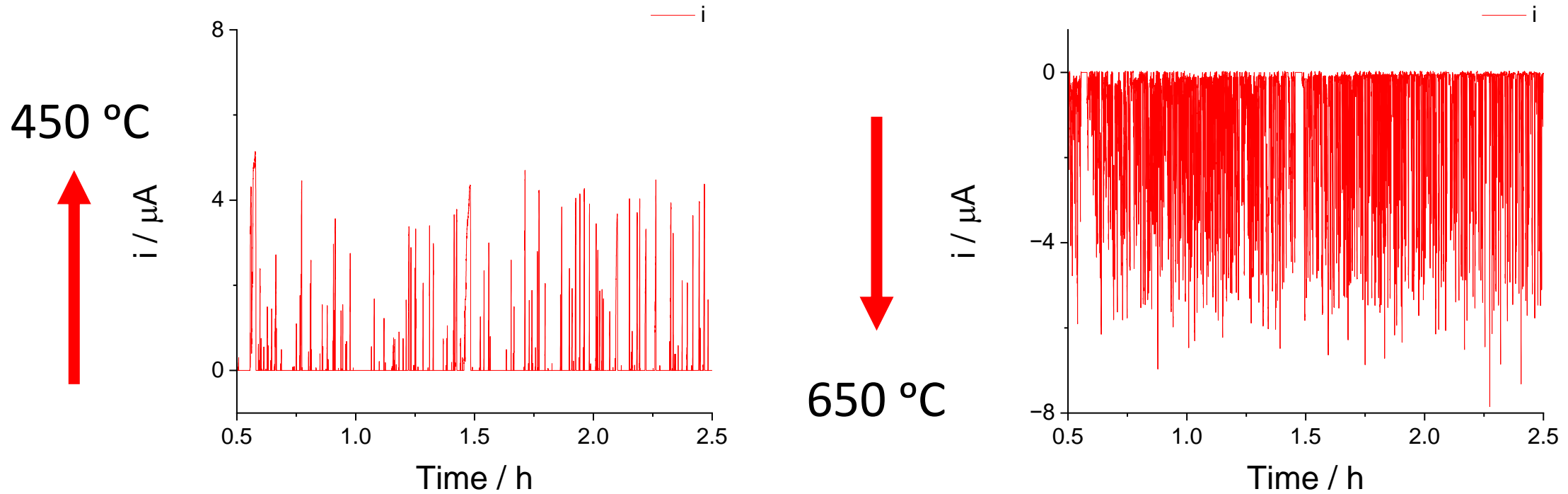
- More frequent metastable events on 650 °C compared to 540 °C

650 °C
↑
540 °C

650 °C (WE1) + 540 °C (WE2)



Comparison of Pitting Susceptibility via Electrochemical Noise



- Transients were split into positive and negative
- Frequency analysis was conducted on the transients

Comparison of Pitting Susceptibility via Electrochemical Noise

- Metastable events more frequent on microstructure with higher ageing temperature (650°C)
- Results indicate pit initiation easier on 650°C microstructure – would also suggest this microstructure is more likely to develop stable pits

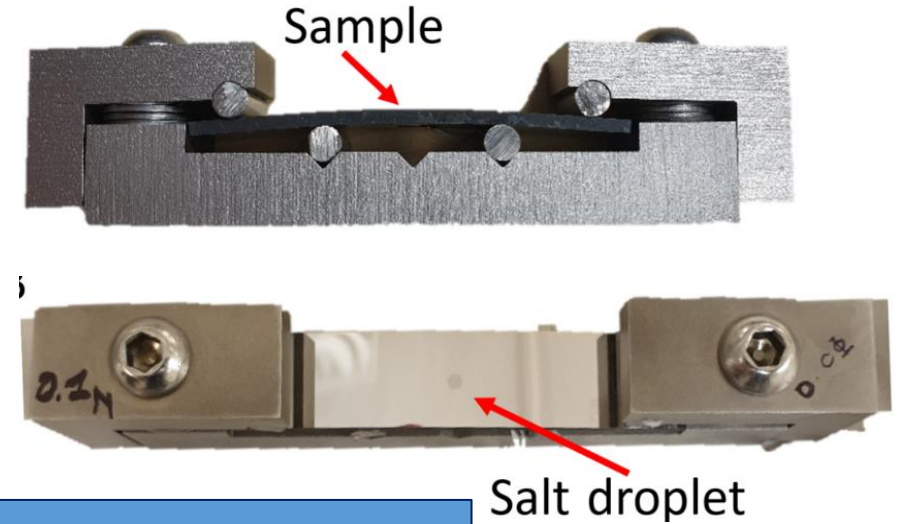
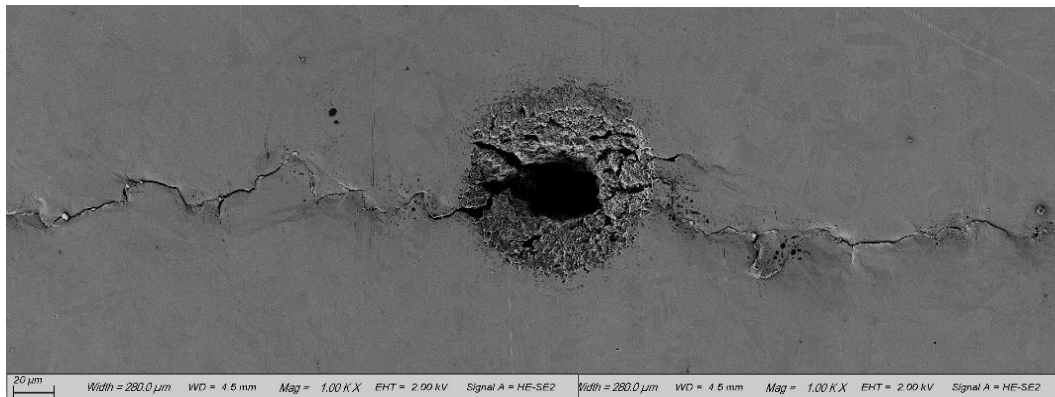
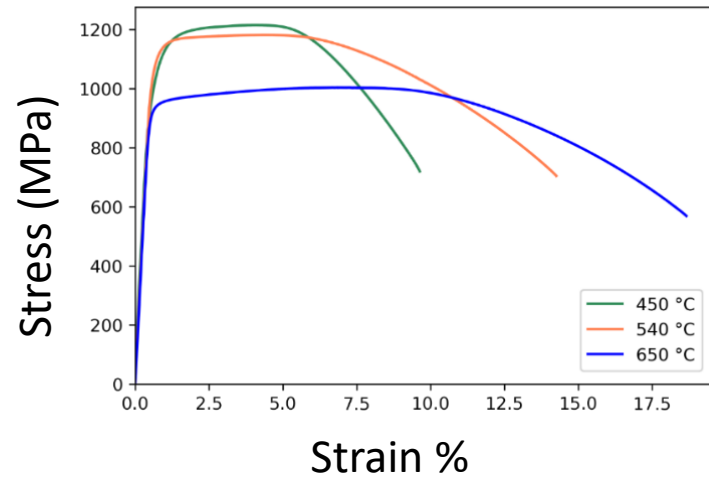
Likely pitting susceptibility:
650 °C > 540 °C > 450 °C

	Frequency of events / Hz		
Galvanic Couple	450 °C	540 °C	650 °C
450_650 (650GRD)	4×10^{-3}		3×10^{-2}
450_540 (540GRD)	3×10^{-3}	2×10^{-2}	
540_650 (540GRD)		1.5×10^{-2}	5×10^{-2}

Susceptibility to Environmentally Assisted Cracking

Testing method allows:

- Investigation of microstructure effect on SCC
- Study of pit to crack transition
- Investigation of cracking behaviour



Test details:

- Stress applied via 4-point bend to 80% YS of 540 °C sample
- 1 µl MgCl₂ salt deposits with concentrations 1M, 0.1 M or 0.01 M
- Temp = 50 °C, Time = 5 and 10 day
- Pit diameter and crack length measured post test
- Stress-free specimens tested under identical conditions

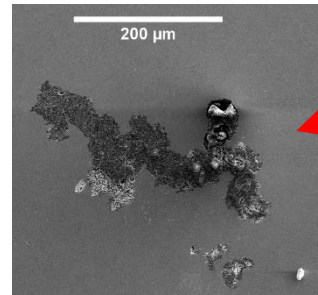
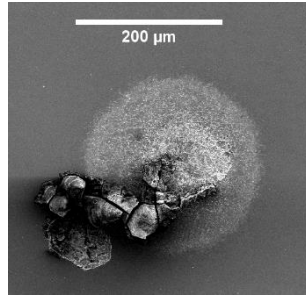
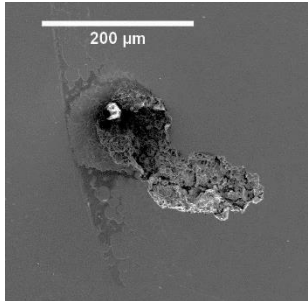
Corrosion Morphology (Non-Stressed Specimens)

10 Days

450 °C

540 °C

650 °C

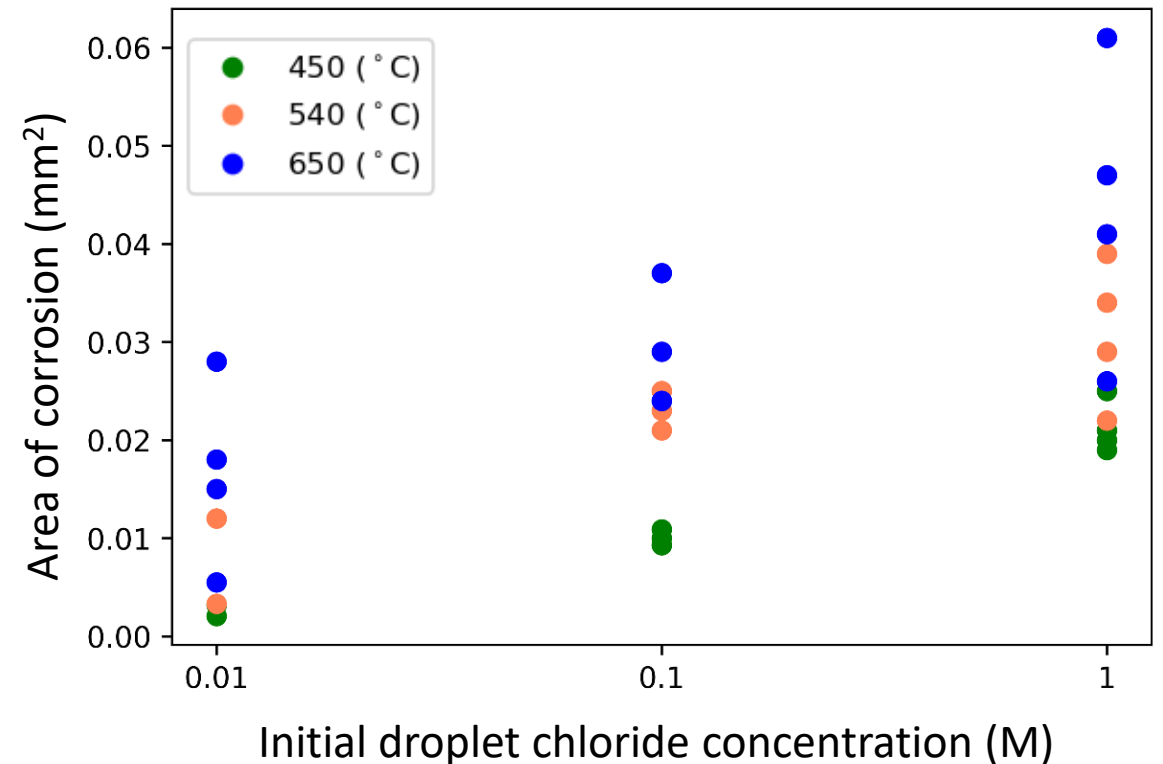


Area of corrosion pits measured and plotted for each ageing temperature

Experimental Conditions

- 1 μl droplet from 1M MgCl_2
- Temperature – 50 °C
- RH – Saturated MgCl_2 ca. 30%
- Stress – 0 MPa

- Area of corrosion increases with initial droplet concentration – likely due to higher surface area remaining for higher concentrations
- 650 °C has largest area of corrosion – suggests pit initiation time is smaller compared to 450 °C and 540 °C

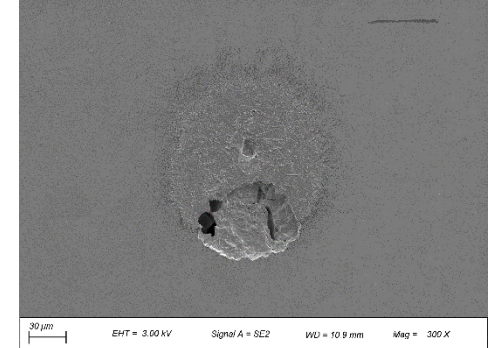
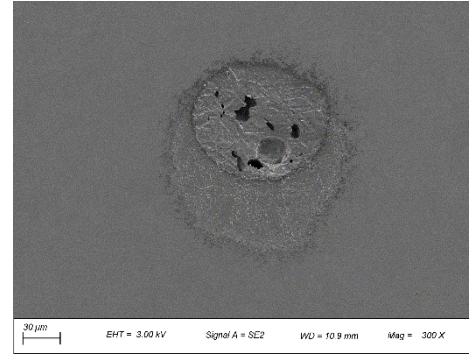
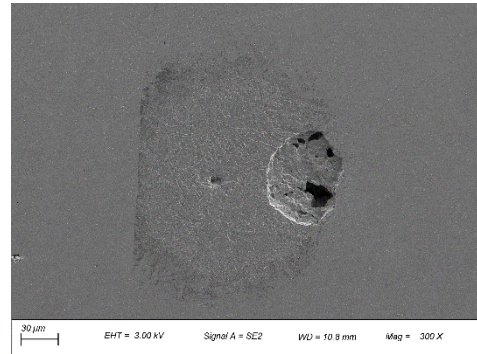
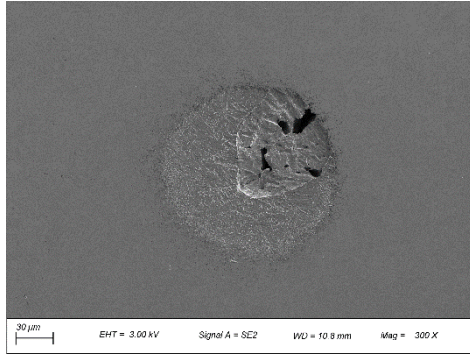


Atmospheric Corrosion - 1M MgCl₂

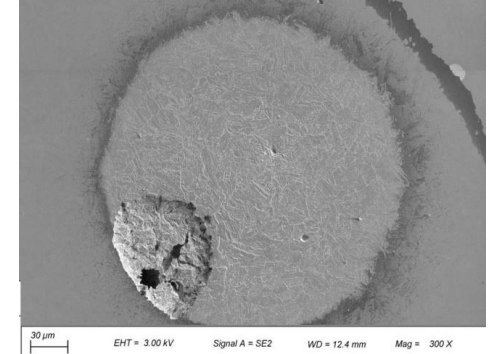
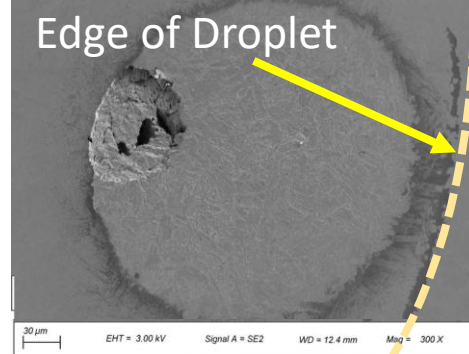
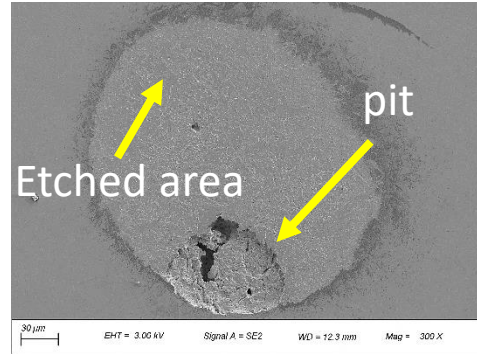
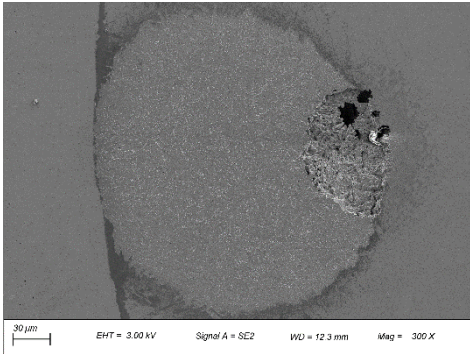
- Time – 10 days
- Samples tested without stress

- RH ~ 90% - 1M MgCl₂
- 50 °C

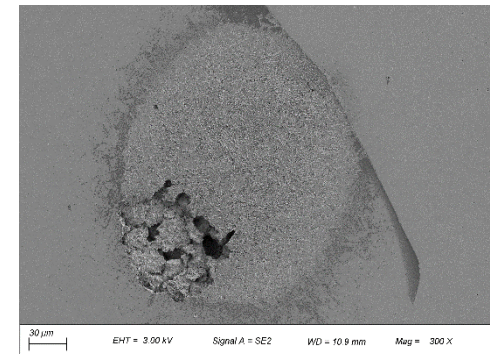
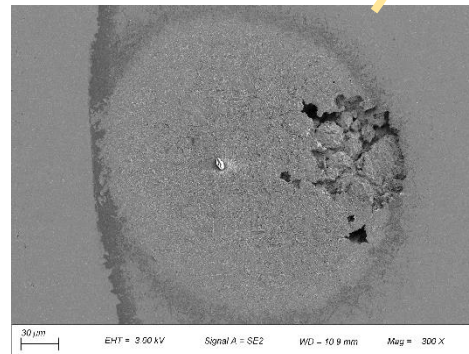
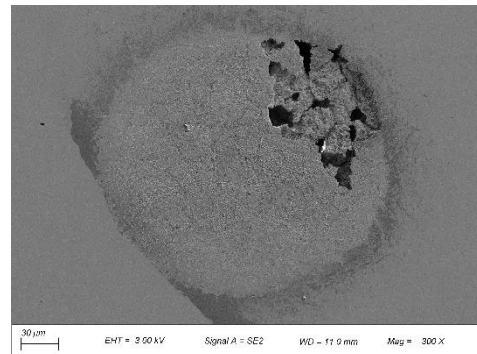
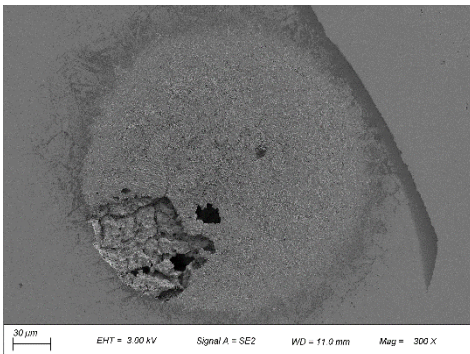
450 °C



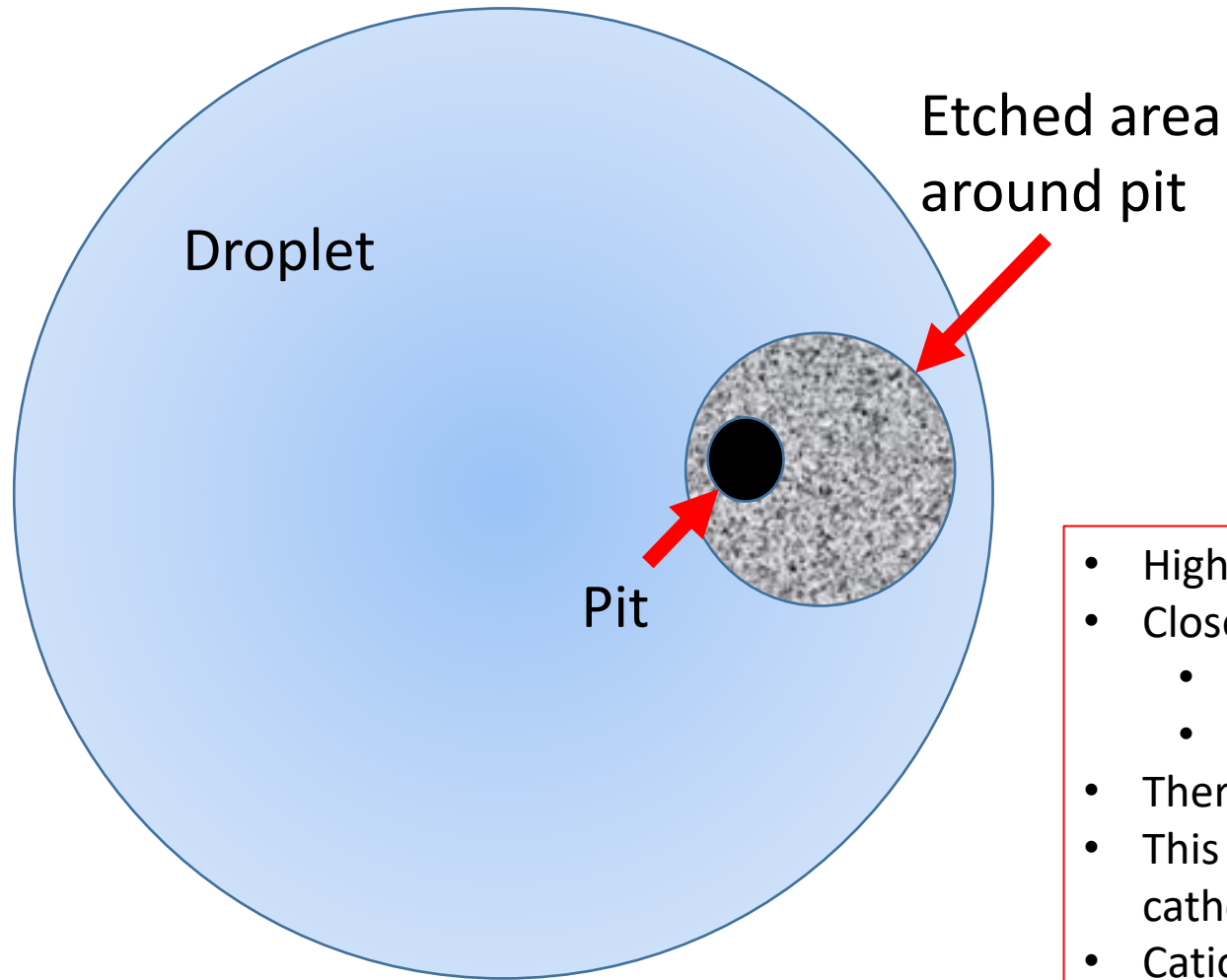
540 °C



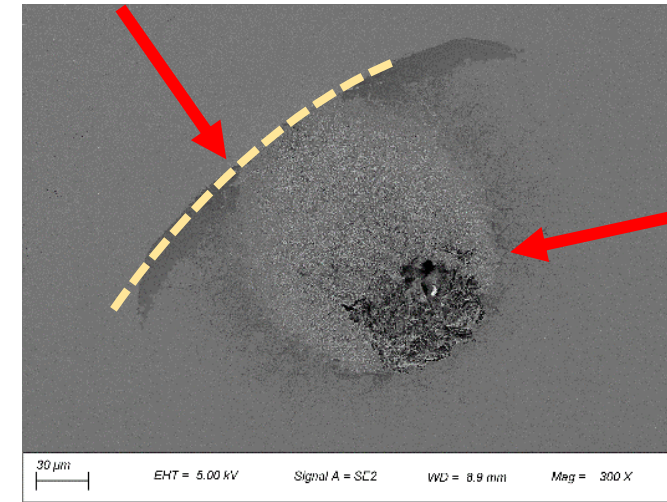
650 °C



Droplet Etching in Pit Viscinity



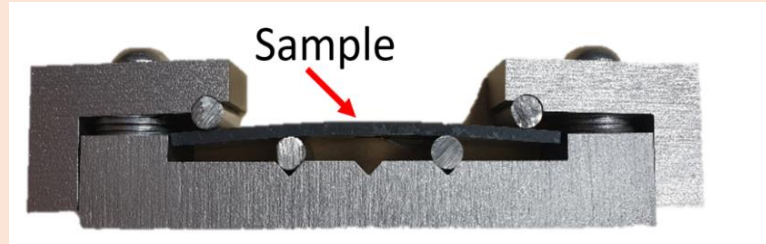
Edge of Droplet



Pits nucleate near edge of droplet with etched area around them

- Higher pH near edge of droplet
- Close to the middle there is:
 - Low oxygen
 - Low Cathodic activity
- Therefore potential is higher near the edge
- This causes the pit to nucleate near edge as it needs cathodic activity to support
- Cations are created within pit and migrate to cathode (near edge) which causes local acidification and therefore etching of area shown

EAC in Four-Point Bend Specimens



Stressed samples with
MgCl₂ salt droplet

Cleaning

Samples analysed post test with
SEM to understand extent of SCC



Experimental Conditions

- 1 μ l droplet from 1M MgCl₂
- Temperature – 50 °C
- RH – Saturated MgCl₂ - 30%

EAC in Four-Point Bend Specimens

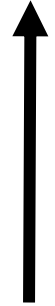
450 °C

Time = 5 days

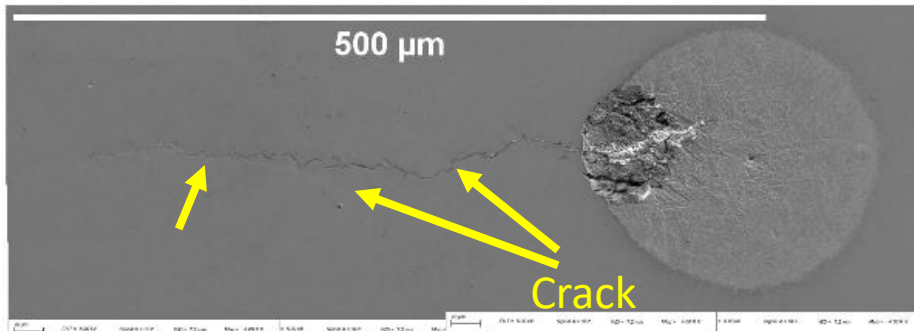
Experimental Conditions

- 1 μl droplet from 1M MgCl_2
- Temperature – 50 °C
- RH – Saturated MgCl_2 - 30%

σ

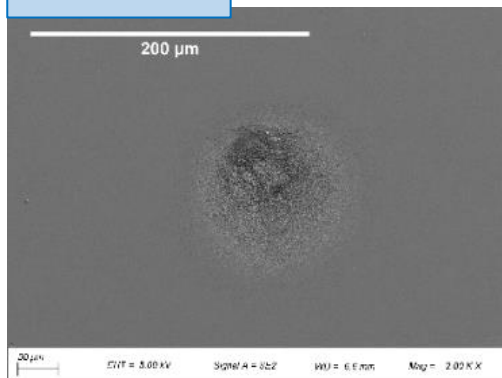


540 °C



650 °C

σ



- All samples susceptible to localised corrosion under conditions tested
- Cracks observed on material aged at 450 °C and 540 °C
- Extent of corrosion on 540 °C is greater than that on 450 °C
- No cracks in material aged at 650 °C

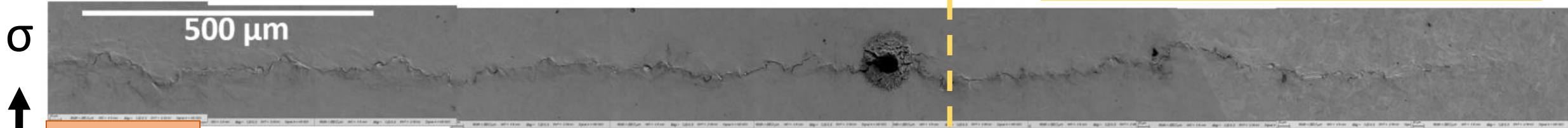
EAC in Four-Point Bend Specimens

450 °C

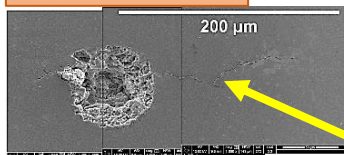
10 days

Experimental Conditions

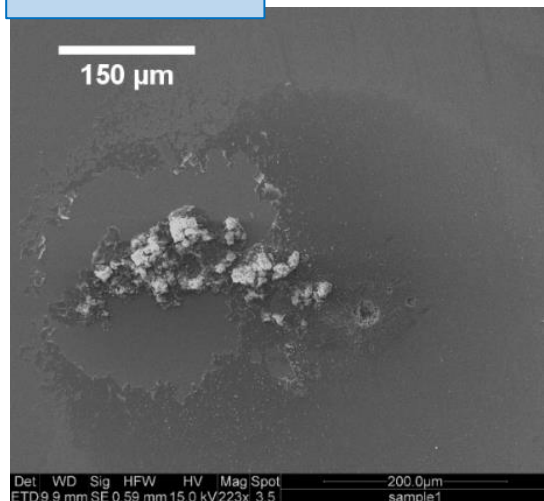
- 1 μl droplet from 1M MgCl_2
- Temperature – 50 °C
- RH – Saturated MgCl_2 ca. 30%



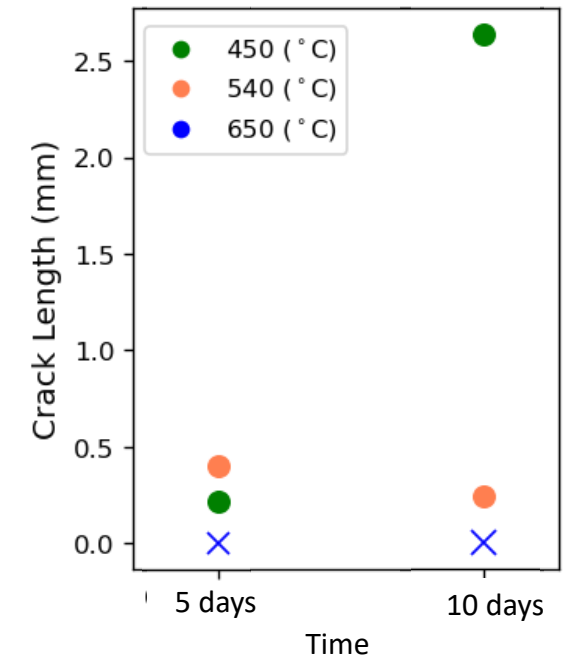
540 °C



650 °C

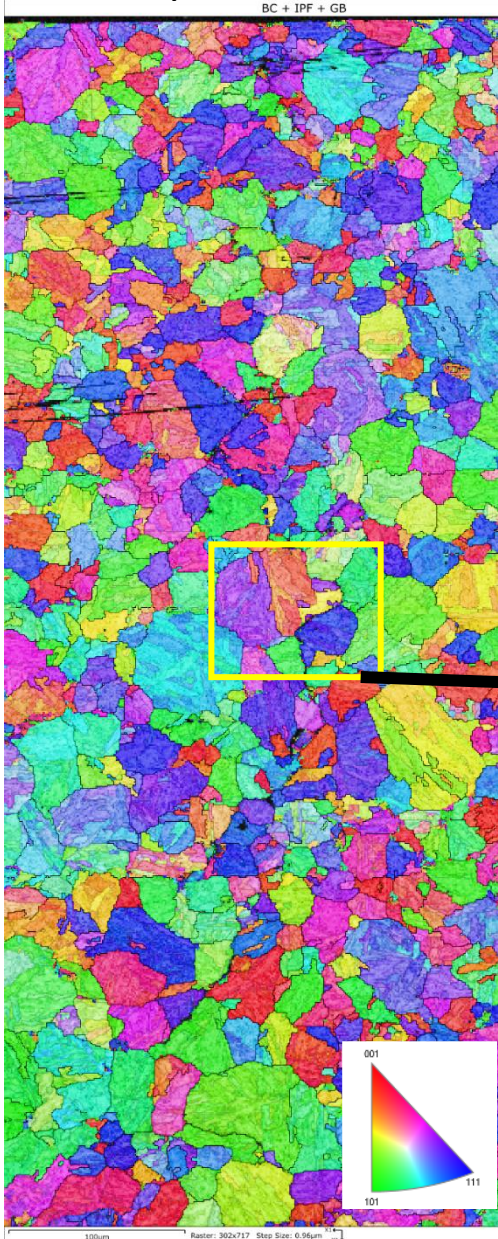


- Long cracks seen material aged at 450 °C
- Shorter cracks seen in 540 °C
- No cracks in material aged at 650 °C under the conditions tested



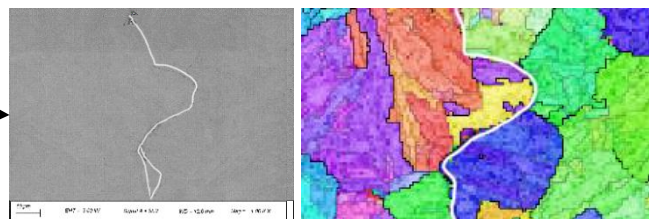
Crack Pathway as a Function of Ageing Temperature

Sample surface



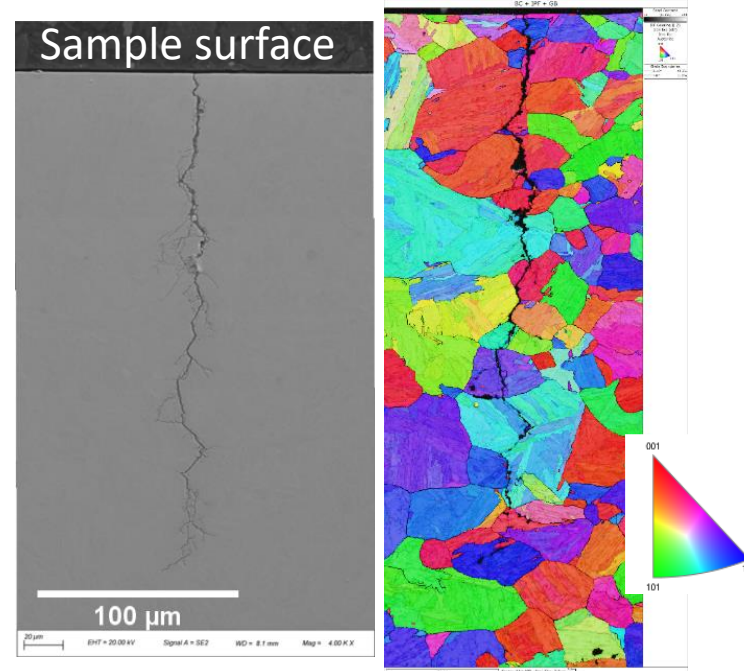
450 °C

- 450 °C – thin crack travels along PAGB (Pathway entirely IG)
- Suggests decohesion and susceptibility to HE



PAGBs reconstructed using AztecCrystal parent grain analysis

540 °C

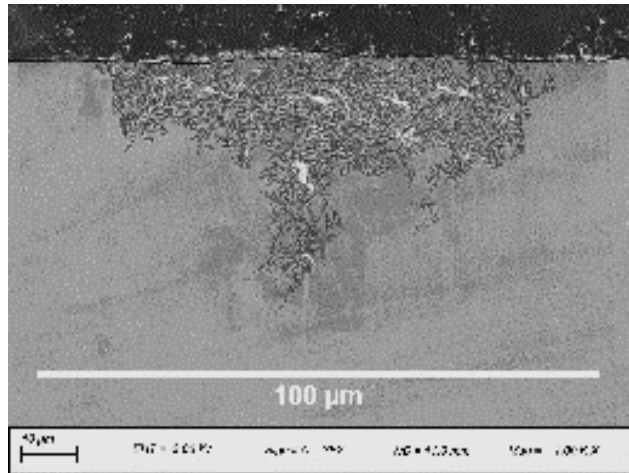


- Crack travels through some grains for 540 °C – mixture of TG and IG cracking
- Possible Cl induced SCC

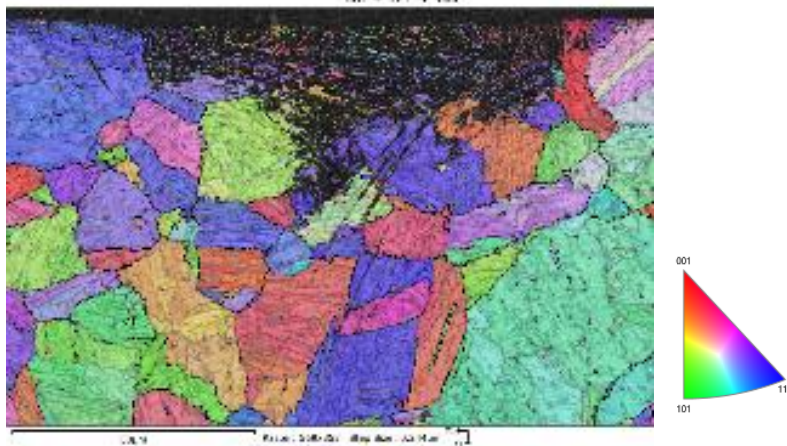
Crack Pathway as a Function of Ageing Temperature

650 °C

PAGBs reconstructed using AztecCrystal parent grain analysis



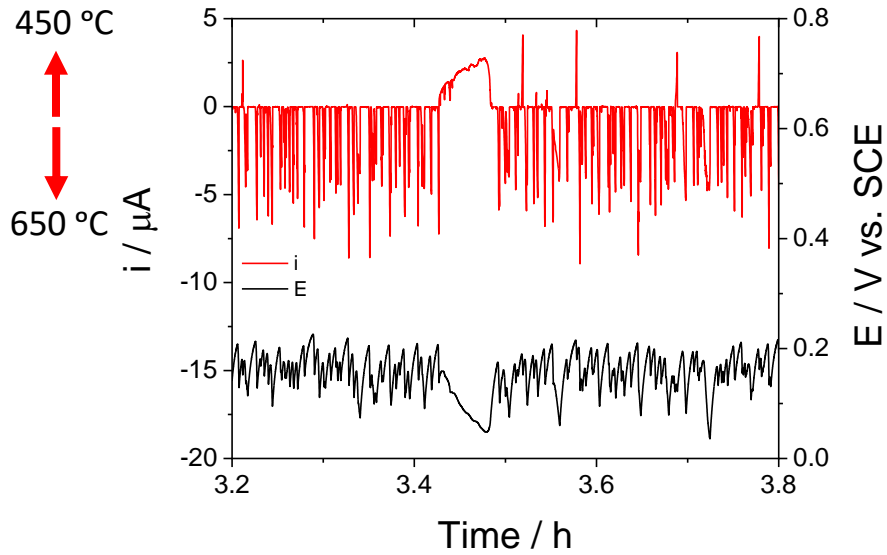
Sample surface



- Dish shaped pit - large area of corrosion near surface. No cracking
- Possibility that pit is fast growing
- Initiation time required for pit to crack transition not reached

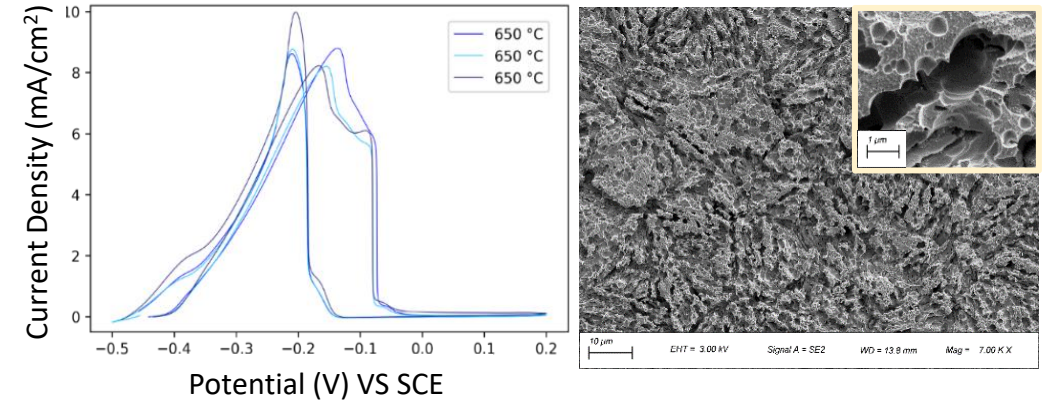
Summary and Conclusions

- Electrochemical investigations indicate 650 °C microstructure is most susceptible to pit initiation & most resistant to environmentally assisted cracking

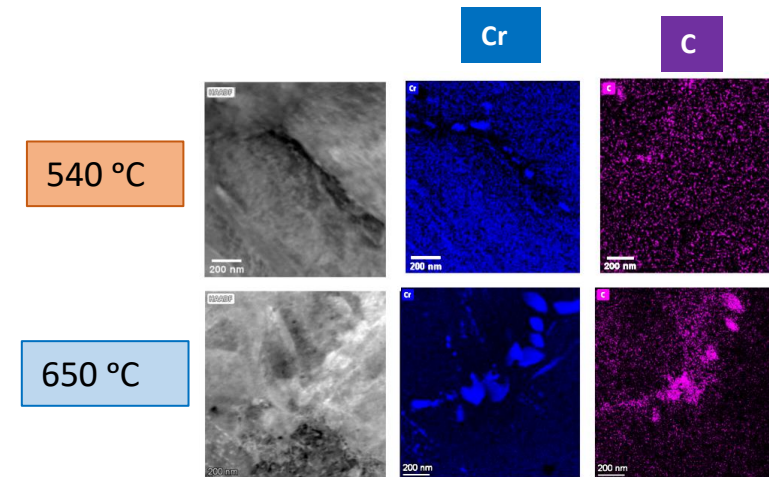


- Greater frequency of metastable events indicates more susceptible pitting sites on 650 °C

- High DOR for 650 °C found through DL-EPR – may explain high frequency of pit initiation



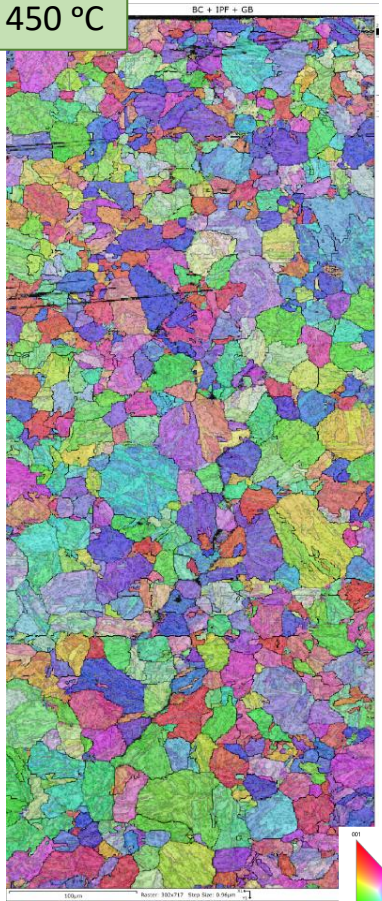
- Susceptible sites likely related to Cr depleted zones associated with Cr Carbide formation or lower Cr content in reverted austenite



Summary and Conclusions

Susceptibility to EAC decreases with increasing ageing temperature – opposite to pit susceptibility

450 °C



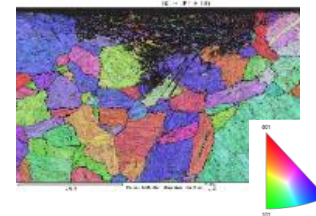
- Pit initiation time is longest (metastable pit frequency low with long lived events) for 450 °C microstructure
- Microstructure very susceptible to cracking – IG pathway suggests a mechanism involving decohesion via HE

540 °C



- 540 °C susceptible to cracking but mechanism may be Cl⁻ induced SCC indicated by TG crack pathway

650 °C



- 650 °C develops large dish-shaped pits transition to cracking does not occur
- Initiation time associated with pit-to-crack transition may not have been reached
- Presence of austenite may inhibit cracking – due to lower mechanical driving force

Thank you for Attending our Joint Meeting.
Any Questions?

Contact:

Email: Alyshia.Keogh@Manchester.ac.uk

LinkedIn



Acknowledgments: Financial support by Airbus, EPSRC and Henry Royce Institute (grant EP/R00661X/1 and EP/P025021/1) for access to electron microscopes
Material supplied by Aubert and Duval